



Issue:	1
Date:	21. September 1999
Page:	i

# CryoSat

## Science and Mission Requirements

**Edited by:**

**Prof. Duncan Wingham**  
**Lead Investigator**

•  
Department of Space & Climate Physics  
University College London  
17-19 Gordon St.  
London WC1H 0AH

•  
21. September 1999

		Issue: 1 Date: 21. September 1999 Page: ii
---	--	--

## Acknowledgements



This document borrow heavily from the proposal "CryoSat: A Mission to Determine Fluctuations in the Mass of the Earth's Land and Marine Ice Fields". The Lead Investigator would like to acknowledge the implicit contribution of the authors of the CryoSat proposal. These were in addition to the Lead Investigator: Giovanni Angino, Alenia Aerospazio, Italy, Prof. Reinhard Dietrich, Technical University of Dresden, Germany, Dr. Rene Forsberg, National Survey & Cadastre, Denmark, Dr. Alan Haskell, Defence Research Agency, UK, Dr. Karen Heywood, University of East Anglia, UK, Prof. Ola Johannessen, Nansen Centre, Norway, Dr. Seymour Laxon, University College London, UK , Prof. Peter Lemke, Institute of Marine Research, Germany, Dr. Mikko Lensu, University of Helsinki, Finland, Uwe Mallow, Dornier Satellitesysteme GmbH, Germany, Laurent Phalippou, Alcatel Space Industries, France, Prof. Giovanni Picardi, University of Rome 'La Sapienza', Italy, Prof. Christian Tscherning, University of Copenhagen, Denmark, Prof. Keith Raney, Johns Hopkins University, USA, Dr. Stein Sandven, Nansen Centre, Norway, Dr. Remko Scharroo, Delft Institute for Earth Oriented Research, Netherlands , Dr. Hans Werner Schenke, Alfred Wegener Institute, Germany, Dr. David Vaughan, British Antarctic Survey, UK, and Nick Veck, National Remote Sensing Centre Ltd., U.K..

## Table of Contents



<b>1 Introduction &amp; Summary .....</b>	<b>1</b>
<b>2 Scientific Context of the CryoSat mission .....</b>	<b>2</b>
2.1 The Importance of the Cryosphere .....	2
2.1.1 The Cryosphere and Climate .....	2
2.1.2 The Cryosphere and Sea Level. ....	4
2.2 The Principal Scientific Questions .....	5
2.2.1 Climate Uncertainties.....	5
2.2.2 Sea Level Uncertainties.....	6
2.3 Dealing with Uncertainties: Earth System Modeling .....	7
2.3.1 Coupled Ocean-Atmosphere-Ice Modeling.....	7
2.3.2 Coupled Ice-Sheet Ocean Solid-Earth Modeling.....	8
2.4 Dealing with Uncertainties: Observational Demands .....	9
2.4.1 Sea Ice Thickness and Mass. ....	9
2.4.2 Ice Sheet, Ice Caps and Glacier Mass Imbalance. ....	11
2.5 The Contribution to Earth Explorer and other International Programs.....	13
2.5.1 Relevance to ESA Earth Explorer Objectives.....	13
2.5.2 Complementarity with ERS, ENVISAT and Earth Explorer Core Missions. ....	13
2.5.3 Complementarity with Other Missions. ....	14
2.5.4 Complementarity with Climate Change Programs.....	15
<b>3 General Mission Characteristics.....</b>	<b>15</b>
3.1 Scientific Objectives of the CryoSat Mission .....	15
3.1.1 Primary and Secondary Mission Goals.....	15
3.1.2 Overview of Science and Measurement Requirements. ....	16
3.2 The Measurement of Thickness and Mass Variations. ....	18
3.3 Natural Variability in Ice Mass and Density and Atmospheric Refraction .....	20
3.3.1 Sea Ice Mass Variability. ....	20
3.3.2 Land Ice Mass Variability .....	21
3.4 The Measurement Requirements .....	23
3.4.1 Coverage, Mission Duration and Measurement Accuracy. ....	23

---

3.4.2 Horizontal Resolution.....	24
3.4.3. Spatial and Temporal Sampling.....	25
3.4.4 Spatial Extent. ....	25
3.5 Mission Timing. ....	26
<b>4 Technical Concept .....</b>	<b>27</b>
4.1 The Radar Altimeter. ....	27
4.1.1 Instrument Concept and Parameters. ....	27
4.1.2 Elevation Retrieval. ....	29
4.1.3 Altimeter Precision and Surface Roughness. ....	32
4.2. Measurement Error Budget .....	33
4.2.1 Sea Surface Topography Uncertainty .....	33
4.2.2 Atmospheric Refraction Uncertainty.....	34
4.2.3 Orbit Error. ....	34
4.2.4 Orbit Pattern and Vertical Accuracy .....	35
4.3 Echo windowing requirements. ....	37
4.4 Radiometric and Fidelity Requirements. ....	39
4.4.1 Range of Backscattering Coefficient and Dynamic Range.....	39
4.4.2 Echo Fidelity.....	40
4.5 Verification Activities.....	41
4.6 Data Product Requirements .....	43
<b>5. Bibliography.....</b>	<b>45</b>

		<div>Issue: 1</div> <div>Date: 21. September 1999</div> <div>Page: v</div>
---	--	--

## Change Record

		Issue: 1 Date: 21. September 1999 Page: 1
---	--	---

## 1 Introduction & Summary

This document describes the CryoSat mission. It aims to provide the scientist and the engineer with an explanation of the importance of the mission, and the basis for the design of the CryoSat satellite and instrument payload. It is organised into four sections. § 2 describes the scientific background and context of the mission, and describes why the data the mission provides are important. § 3 describes the scientific objectives of the CryoSat mission, and derives from these the measurement requirements. § 4 explains the instrument concept, and illustrates how the measurements of the instrument payload will provide the information the science requires. Finally, in § 5, is a bibliography.

*§ 2 Scientific Context.* The cryosphere has a central role in the Earth's radiation budget. Loss of sea ice is predicted to cause a larger greenhouse-gas warming in the Arctic than the rest of the Earth. Ice sheets and glaciers are a control on sea level. They are the largest uncertainty in the sources of present sea level rise. The central questions concerned with cryosphere are: How is the deepwater formation and polar and sub-polar ocean exchange affected by sea ice? What are the imbalances of the Antarctic and Greenland Ice Sheets? Ocean-atmosphere-ice models, and ocean-ice-solid-Earth models, demand spatially- and temporally-continuous estimates of ice mass fluxes at regional and global scales. Present observations are deficient. Only satellites will make good the deficiency. CryoSat and International Programmes will provide a decade of focussed study of the roles of the cryosphere.

*§ 3 General Mission Characteristics.* The scientific requirements demand CryoSat measure variations in the thickness of perennial sea and land ice fields to the limit allowed by natural variability, on spatial scales varying over three orders-of-magnitude. The natural variability of sea and land ice depends on fluctuations in the supply of mass by the atmosphere and ocean, and snow and ice density. CryoSat measurement requirements are determined from estimates of these fluctuations. Continuity in time and space with other satellites make 2003 the optimal launch date.

*§ 4 Technical Concept.* The addition of a synthetic aperture and interferometry to the ENVISAT or Poseidon altimeters provides an altimeter to meet the measurement objectives. Preliminary analysis of the error budget of the CryoSat concept indicate the measurement requirements can be met. The range of parameters CryoSat will observe is determined from the character of the Earth's ice surfaces. Geophysical verification of the CryoSat data will be performed in the Arctic and Antarctic. Modifications to the existing ENVISAT altimeter data processing can provide CryoSat processing to level 1b.

## 2 Scientific Context of the CryoSat mission

This section describes the scientific background to the CryoSat mission. It attempts, in so far as this is possible, to isolate questions of particular importance to contemporary thinking concerning the role of the cryosphere. The way in which these may be dealt with by models is described, together with the need that arises for CryoSat experimental measurements. The role of the CryoSat mission within the wider context of international programmes of polar and climate research is outlined.

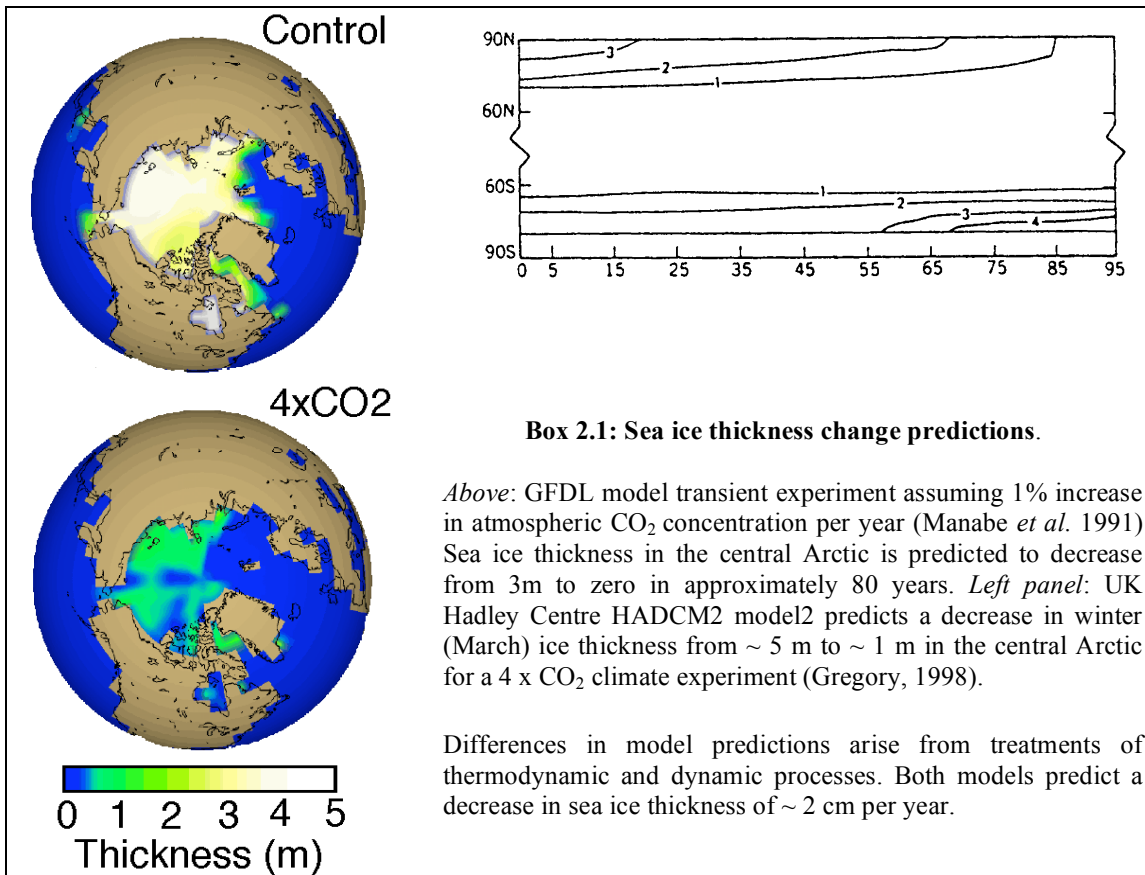
### 2.1 The Importance of the Cryosphere

#### 2.1.1 The Cryosphere and Climate

The Earth's Quaternary climate has been characterised on time-scales of 100,000 years by interlinked changes in temperature, CO<sub>2</sub>, ice sheets and sea level. More rapid global changes exposed in ice-core and other paleo-records also appear related to fluctuations in the cryosphere (Bond *et al.* 1993). In contrast, interannual fluctuations in the modern climate reflect ocean-atmosphere interactions whose source is the tropical Pacific but whose influence extends to the poles (Horel & Wallace 1981). Between these extremes lie fluctuations we poorly understand on a great range of time-scales. At the core of this uncertainty is our limited knowledge of the interactions of the cryosphere and atmosphere with the ocean thermohaline circulation.

In the modern climate, the ocean circulation is responsible for some half of the poleward heat transport, the remaining half being contributed by the atmosphere (Peixoto & Oort 1992). The release of heat from ocean to atmosphere in winter serves to maintain atmospheric temperature: mild winters in north west Europe are a consequence. By the time warm water originating from the Gulf Stream has reached northern Europe and the Nordic Seas, the surface water has given up most of its heat to the atmosphere and becomes dense enough to sink in winter through deep convection. Surface waters are replaced by a fresher (and thus lighter) supply from the polar cryosphere. In some years these can form a fresh cap preventing deep convection (Aagaard 1994).

Trends in the supply of freshwater from the cryosphere may profoundly affect the thermohaline circulation. Rapid and large changes in temperature are observed in the paleo-record at times of increased discharge from the Northern Hemisphere Ice Sheets (Broecker 1994). Coupled models show a decline in the Northern Hemisphere poleward transport in response to increased freshwater supply (Manabe and Stouffer 1988), and/or greatly increased latitudinal variability (Weaver & Sarachik 1993). Such changes will have greatest impact on areas such as Europe that presently experience warm winter temperatures.





75% of the Earth's net outgoing radiation occurs between the latitudes of 50° and 70° (Peixoto & Oort 1992). These regions are characterised by a seasonal marine and land cryosphere with highly reflective surfaces. A reduction in their extent or persistence, as will occur in a warming atmosphere, affects the atmospheric radiation balance. Decreased ice cover results in an increase in the summer storage of heat by the ocean, and its release into a thus further-warmed polar atmosphere in winter. Regional warming of the Arctic in winter by 4 °K or more is the largest predicted consequence of increased CO<sub>2</sub> emission (Box 2.1; see also *e.g.* Coleman *et al.* 1995, Murphy & Mitchell 1995). Whether this response is due to physical feedbacks or to the simplified sea ice in climate models is a focus of the Climate Variability and Program (WCRP 1998) and Arctic Climate System Study (WCRP 1992).

Arctic sea ice is sensitive to small changes in vertical oceanic heat flux<sup>1</sup>. The salinity-stratified upper layers of the Arctic Ocean admit little vertical exchange of heat and salt. Perturbations in this structure, allowing heat exchange with deeper water, may lead to radically different sea ice cover (see *e.g.* Maykut & Untersteiner 1971). Brine expulsion makes sea ice fresher than sea-water. Its wind-driven transport from the Arctic Ocean accounts for approximately of the freshwater budget of the Greenland Sea (Aagaard & Carmack 1989), the principal site of the overturning of the thermohaline circulation in the

<sup>1</sup> A flux of 10 W m<sup>-2</sup> will melt ~ 1 m of ice in 1 year.



		Issue: 1 Date: 21. September 1999 Page: 4
---	--	---

Northern Hemisphere. Variations in Arctic sea ice may have profound consequences for the poleward transport of heat by North Atlantic.

The circulation of the Southern Ocean is dominated by the zonal Circumpolar Current, which isolates the Antarctic continent and maintains its low temperature. On the other hand, the seasonal salinity-forcing of sea ice formation and melting south of the Circumpolar Current; the melting of glacier ice, either *in-situ* or from icebergs calved from the ice sheet; combined with the intense winter cooling of the surface that occurs through breaks (“polynyas”) in the pack ice, creates the dense Antarctic Bottom Water that spreads off the continental shelf, under the Circumpolar Current, and forms much of the bottom water in the Pacific, Indian and Atlantic Oceans. The freshwater and heat fluxes change episodically. The mid-1970s formation of Weddell Sea Polynya (Zwally *et al.* 1983) and the collapses of the Antarctic Peninsula ice shelves (Rott *et al.* 1996) are recent examples. Little is known of the variability of these episodes, or their consequence on the thermohaline circulation.

### 2.1.2 The Cryosphere and Sea Level.

On time-scales of 10,000 years, fluctuation of ice sheets in the Northern and Southern Hemispheres has dominated variations in global sea level<sup>2</sup>. From 18,000 years ago, sea level rose globally by 90 m as a result of the retreat of the Laurentide, Greenland and Scandinavian Ice Sheets (Peltier 1988). This rise in sea level initiated, presumably, a shrinking of the marine Antarctic Ice Sheet, adding perhaps another 30 m to sea level (Nakada & Lambeck 1988). This retreat appears to have been completed 5000 years ago. Since that time, sea level appears to have been stable, varying by perhaps 10 cm, until the last century (Varekamp *et al.* 1992). Since then, the rate appears to have accelerated, with a rise of ~ 15 cm over the past 100 years (Gornitz *et al.* 1982).

The smallness of sea-level rise makes its explanation a challenge. The rate of 20<sup>th</sup> century rise is equivalent to the addition of 0.5 Tt yr<sup>-1</sup> of water. In comparison, the ocean annually exchanges 361 Tt yr<sup>-1</sup> with the atmosphere, and 99 Tt yr<sup>-1</sup> with the land (Peixoto and Oort, 1992). The rise is small, and may be explained by a number of competing geophysical processes, each of which is a complex process in its own right. These include tectonics; the redistribution of water from ice sheet and glacier retreat, the rebound of the lithosphere and mantle; the affect of these on the Earth’s gravitational field; the thermal expansion of the ocean; the extraction of ground water; and changes in coastal sedimentation and erosion.

Nonetheless, the cryosphere is the largest potential source of sea level fluctuations. It contains ~ 90% of the Earth’s freshwater, largely in the Antarctic Ice Sheet. Some glaciologists (Thomas *et al.* 1979, Hughes 1981) have questioned the stability of the West Antarctic Ice Sheet, which contains sufficient water to change sea level by 5 m. However, fluctuations of individual drainage basins are all that is needed to explain the 20<sup>th</sup> century rise, which corresponds to ~ 0.2% of Antarctic Ice Sheet mass. Little is known about fluctuations in ice sheets on this time-scale. The fast-flowing Antarctic ice streams, transporting ice from the interior, show a variety of dynamic behaviour, and evidence of

---

<sup>2</sup> In this proposal, sea level means sea depth. The locus of points with zero sea level is the coastline.

change on century scales (Alley & Whillans 1991). Direct observations, variously interpreted, allow the imbalance of the Antarctic and Greenland Ice Sheets to explain all of the present rise, or none of it, or even to be lowering sea level (Warrick *et al.* 1996).

On the other hand, the fact that sea level appears to have accelerated in the last century points towards sources with faster time-constants than those associated with ice sheets. The 20th century sea level rise is equivalent to 25% of the (estimated) mass of small ice caps and mountain glaciers. In this century, glacier retreat has been a notable feature of European and United States glaciers (*e.g.* Haeberli & Hoelzle 1995). The extension of observations of a few glaciers to those of the world at large is fraught with difficulty, but it appears that this may explain 4 cm of the present rise (Meier 1984). Thermal expansion of the ocean associated with global warming is also estimated to have contributed perhaps 4 cm this century (Cubash *et al.* 1992).

Thermal expansion and the melting of ice caps and glaciers are the largest expected sources of 21<sup>st</sup> century sea level rise (Warrick *et al.* 1996). Changes due to global warming in Antarctica and Greenland are modest: increased run-off from the Greenland Ice Sheet may contribute 6 cm; warming of the Antarctic atmosphere may result in a small decrease in sea level through an increase in snowfall. In the longer term the situation is different. Over 1000 years the Greenland Ice Sheet may contribute more than 2 m. Increased melting from the ice sheet is likely to drive its net surface balance close to zero (Wingham 1995 and references therein). Iceberg calving will lower the altitude and surface melting will increase.

## 2.2 The Principal Scientific Questions

### 2.2.1 Climate Uncertainties.



The Arctic is expected to be the region of the Earth most affected by global warming, and changes in the Arctic may have profound implications for the climate around the mid-latitude North Atlantic through alteration of the thermohaline circulation. It is the case today, however, that the principal weapon of prediction, the global atmosphere-ocean-ice climate model, is not yet capable of describing without flux correction (Gates *et al.* 1996) the important mechanisms of climate change in the polar and sub-polar Arctic: Thermohaline circulation and sea-ice formation, transport and decay. Flux corrections themselves depend on knowledge of the mean state. Less is known of the mean state<sup>3</sup> of the polar oceans and their forcings than other oceans, and the spatial and temporal sparsity of observations make a matter of conjecture the statistics of observed variabilities such as the “Great Salinity Anomaly” (Dickson *et al.* 1988) or the Weddell Sea Polynya (Zwally *et al.*, 1983).

Understanding the variation in the thermohaline circulation and its moderation by the cryosphere are large and challenging tasks. They require a better knowledge of the water masses within the Arctic and Southern Oceans, of the variability of their surface forcing,

---

<sup>3</sup> Smith *et al.* (1997) observe that erroneous ocean temperatures in the Levitus (1982) climatology result in the UK Hadley GCM in 0.2 PW of winter atmospheric heating from Hudson Bay alone.

---

		Issue: 1 Date: 21. September 1999 Page: 6
---	--	---

and their exchanges with the sub-polar oceans. Our largest present uncertainties are summarised in the following questions:

- Is the sea ice cover of the Arctic Ocean thinning?
- What is the freshwater balance of the Arctic Ocean? How do variations in freshwater outflow affect deepwater formation and poleward transport of heat by the North Atlantic?
- Is deep water formation in the Southern Hemisphere restricted to the Weddell and Ross Seas? Do the Antarctic Ice Shelves make a significant contribution? Where do transports of deep water occur to the Pacific, Indian and Atlantic Oceans?
- Do open-ocean polynyas play a large role in deep water formation around Antarctica in comparison with brine ejection from sea ice formation? How rapidly are sea-ice forced variations transmitted to the deep water transport to the world's oceans?

These questions require proper treatments in ocean-atmosphere-ice models of the thermohaline circulation, and sea ice dynamics and thermodynamics; a concentration of oceanographic observations in regions of deep water formation; and knowledge of large-scale sea ice mass and thickness budgets. Of these three, the first is a priority in the development of the next generation of IPCC climate models (§ 2.3.1). The second is a principal goal of programs of climate change (§ 2.5.4). The third is a main purpose of the CryoSat.

### 2.2.2 Sea Level Uncertainties.

Sea level rise in the 21<sup>st</sup> century will result primarily from very small changes in the Earth's (very large) reservoirs of water. The prediction of future sea level rise is therefore difficult. Estimates of sea level rise over the 21<sup>st</sup> century vary from 13 to 94 cm (Warrick *et al.* 1996). This spans a range from modest coastline migration to changes with profound political and economic consequences. It is essential that variations in the Earth's stores of freshwater are better determined than at present. The largest uncertainties are associated with the ice sheets, but all sources of sea level rise are in urgent need of better definition. In particular:

- What are the present balances of the Antarctic and Greenland Ice Sheets? Are there regional variations in their mass imbalances? Are the rapid retreats of the Antarctica Peninsula Ice Shelves, or changes in West Antarctic drainage to the Ross Ice Shelf affecting the flow of ice from the deeper interior?
  - Are the large changes in the ice caps and glaciers implied by estimates of their contribution to 20<sup>th</sup> sea level actually occurring? What is the state of balance of the Earth's ice caps and glaciers for which there are no data?
  - Is the "acceleration" in sea level rise over the past 100 years real, or does it reflect a better sampling of the natural variability that followed the widespread introduction of tide-gauges after 1850?
  - What is the uncertainty in the affect of global post-glacial rebound?
-

- Have significant changes in ground water occurred in the 20th century?

These questions involve small changes in mass over large areas of the Earth. Although ground observation may illuminate the physics of the processes involved, satellites are the only method that may constrain mass budgets on the large scale. Of these, ocean altimetry and time-variant gravity are very important and dealt with in § 2.5.2 and § 2.5.3. The mass imbalance of the land ice cryosphere is a goal of the CryoSat mission.

### 2.3 Dealing with Uncertainties: Earth System Modeling

Sea ice, ice sheets and glaciers result from thermodynamic and dynamic interactions between the ice, atmosphere and oceans, and, in the case of land ice, the solid Earth. The complexity of these interactions makes numerical Modeling essential to our understanding of them. In the future, prediction of these systems will involve their simultaneous solution within an “Earth system” model. In the next decade developments in sea ice modeling (§ 2.3.1) will come through global ocean-atmosphere-ice models dealing with annual to centennial variations. Developments in land ice modeling (§ 2.3.2) will integrate models of ice flow with gravitationally self-consistent Earth and ocean models that ignore, for the time being, the dynamical detail of the ocean-atmosphere interaction. This approach is justified because, in the first instance, the time-scales of the processes involved are distinct.

#### 2.3.1 Coupled Ocean-Atmosphere-Ice Modeling.

We have noted in § 1.2.1 that global ocean-atmosphere models are not yet able to reproduce observed sea ice extents in the Northern and Southern Hemispheres, save by using flux corrections (Gates *et al.* 1995). Flux corrections, which essentially hold the sea surface temperature to freezing in regions of climatological sea ice, makes questionable the calculation of the affect of “perturbations” such as CO<sub>2</sub>-induced warming. The physics of sea ice in global coupled models is over-simplified, and recognised as such (Smith *et al.* 1995). They do not contain physics present already in regional sea ice models. With the recognition that variations in themohaline circulation may have important consequences for poleward heat transport, the next decade will see more complete sea ice physics within global ocean-atmosphere ice models.

With the introduction of more realistic sea ice models, it is obvious that observations will be needed to verify them. The lesson from regional sea ice Modeling is that observed *extents* (§ 2.4.1) are of limited value in sea ice model verification. The essential difference between regional models and global models lies in their definitions of ice rheology (Hibler 1979), and thermodynamics which in regional models includes, for example, different thermal and albedo parameterisation of sea ice and snow. Different model rheologies may have different consequences for the longer term evolution of sea ice fields (Grey & Morland 1994) and yet are able to recreate the observed annual cycle of sea ice extent quite accurately (Ip *et al.* 1991, Flato & Hibler 1992, Fischer & Lemke 1994). What is needed to distinguish between rheologies are observations of sea ice thickness. In addition, in climate models, sea ice thickness provides a sensitive verification of the accuracy of atmospheric and ocean heat fluxes. These must be accurate to  $\sim 20 \text{ W m}^{-2}$  to achieve the correct thickness (Fischer &

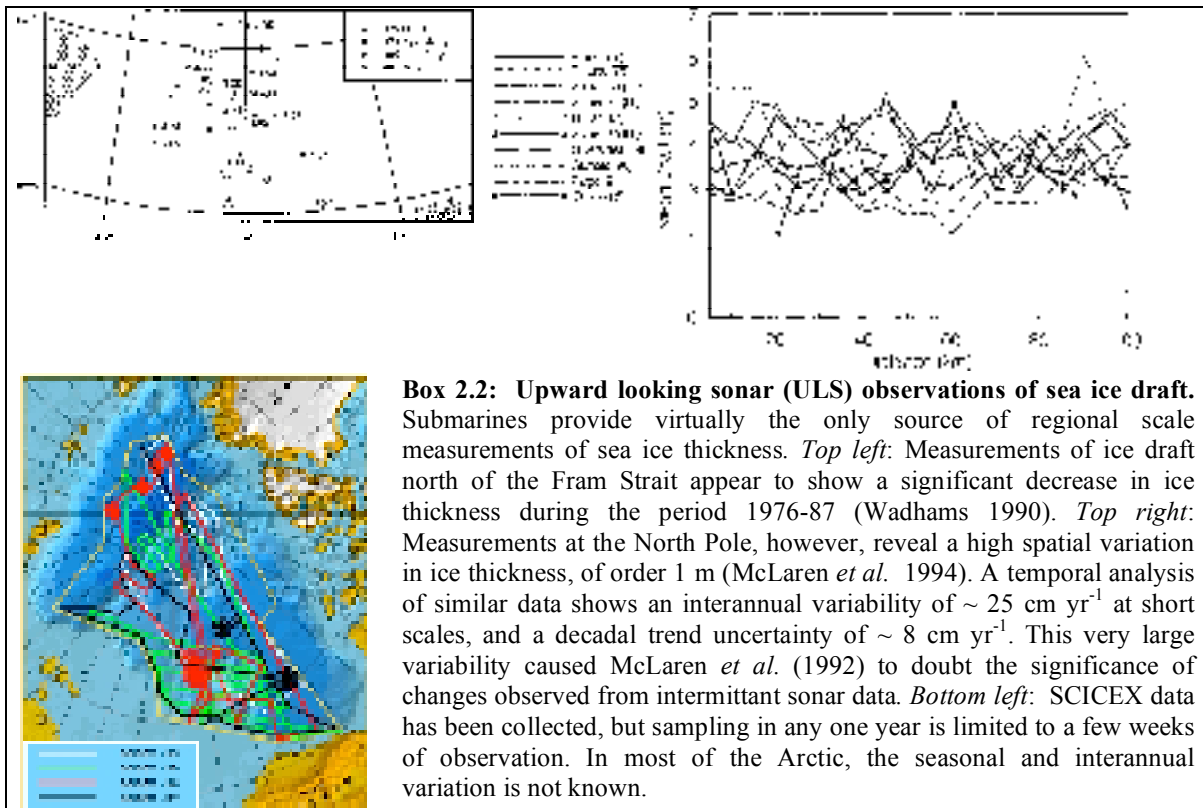
Lemke 1994). Presently, there are few data to compare with atmosphere-ocean-ice models at large spatial scales.

### 2.3.2 Coupled Ice-Sheet Ocean Solid-Earth Modeling.

The collapse of the ice sheets from 20,000 and 5,000 years ago is still observable in the on-going adjustment of the mantle to the redistribution of surface load (Peltier 1988). The most accurate information concerning the Earth's deglaciation history comes from using the ice mass history and relative sea level data as constraints in models of the rebound process (*e.g.* Nakada & Lambeck 1988). The problem is complex, because a mass redistribution at or near the Earth's surface changes the gravitational field, which in turn affects the mass redistribution (Farrel & Clarke 1976). On the other hand, the last decade has seen the development of models of Antarctic and Greenland Ice Sheet history (Huybrechts 1990, Huybrechts 1994) based on laws of ice flow and the estimated history of surface accumulation. These two kinds of models are broadly in agreement.

In the next decade, two developments can be foreseen. Rebound Modeling based on a viscoelastic Earth (Peltier 1974) have shown that the collapse of the glacial forebulge may be significant. For the marine Antarctic Ice Sheet there is good reason to suppose there is coupling between the ice flow and the associated rebound. Although the computer requirements for solving the coupled problem are substantial, developments have already started (Le Meur & Huybrechts 1998). Second, models of Antarctic and Greenland history have yet to include the fast-flowing ice streams that transport 90% of the ice to the coast (Alley & Whillans 1991). These have time-constants that are shorter than those associated with ice flowing through internal deformation. There is theoretical evidence that this type of flow may considerably complicate the deglaciation history of West Antarctica (MacAyeal 1992).

In § 2.1.2 we observed that small relative changes in the Antarctic and Greenland Ice Sheets may have large affects on sea level. The observed extent and thickness, which is all that is available today, provide good constraints on the glacial-interglacial history, but are of limited use to constrain models of present and near-future evolution. Observations are required that test directly the prediction of present rate-of-change of ice mass and its spatial distribution. Huybrechts (1990) predicts a negative imbalance of  $-351 \text{ Gt yr}^{-1}$  for the Antarctic Ice Sheet. Observations that limit the uncertainty to  $\sim 50 \text{ Gt yr}^{-1}$  are needed to provide a challenge to, and sensitive tests for, numerical models. Box 2.5 shows the first such constraints for the Antarctic Ice Sheet. An aim of CryoSat is to extend these observations to the entire ice sheet. Finally, the trend in elevation of an ice sheet is the sum of the trends in ice thickness and isostatic rebound (Wahr *et al.* 1998). Accurate ice sheet elevation rates and time-variant gravity may be important in disentangling the present imbalance from post-glacial rebound. This is considered further in § 2.5.3.



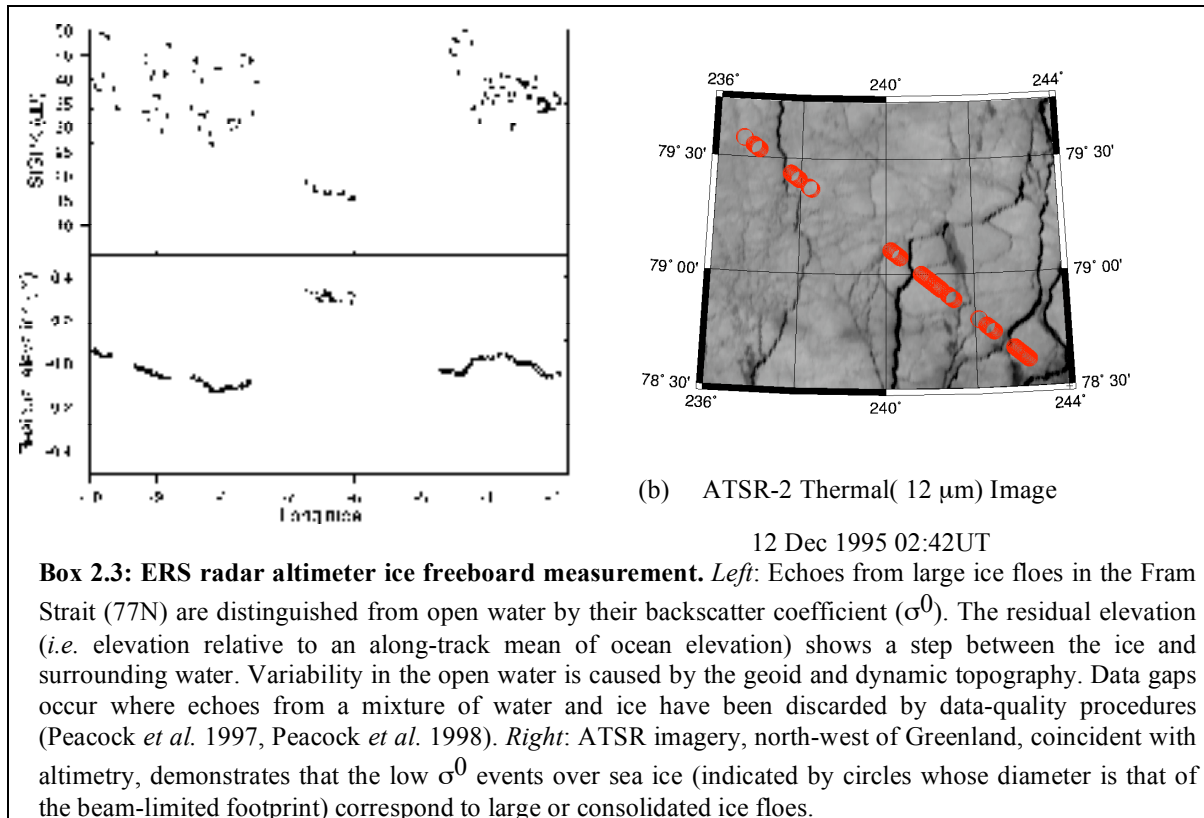
## 2.4 Dealing with Uncertainties: Observational Demands

### 2.4.1 Sea Ice Thickness and Mass.

The measurement of sea ice at large scales is only practical remotely (Box 2.2). This may be done either by measuring sea ice draft using upward-looking sonar (ULS), or by measuring sea ice freeboard using altimetry. ULS measurements are only available from moored arrays or, opportunistically, from submarines. In either case, there are few such measurements. A ULS array operates continuously across the Fram Strait, providing a picture of ice discharge from the Arctic. What is known of interannual variations in Arctic sea ice comes from submarines (Box 2.2). However, ULS is not a practical solution to determine sea ice thickness throughout the Arctic and Southern Oceans.

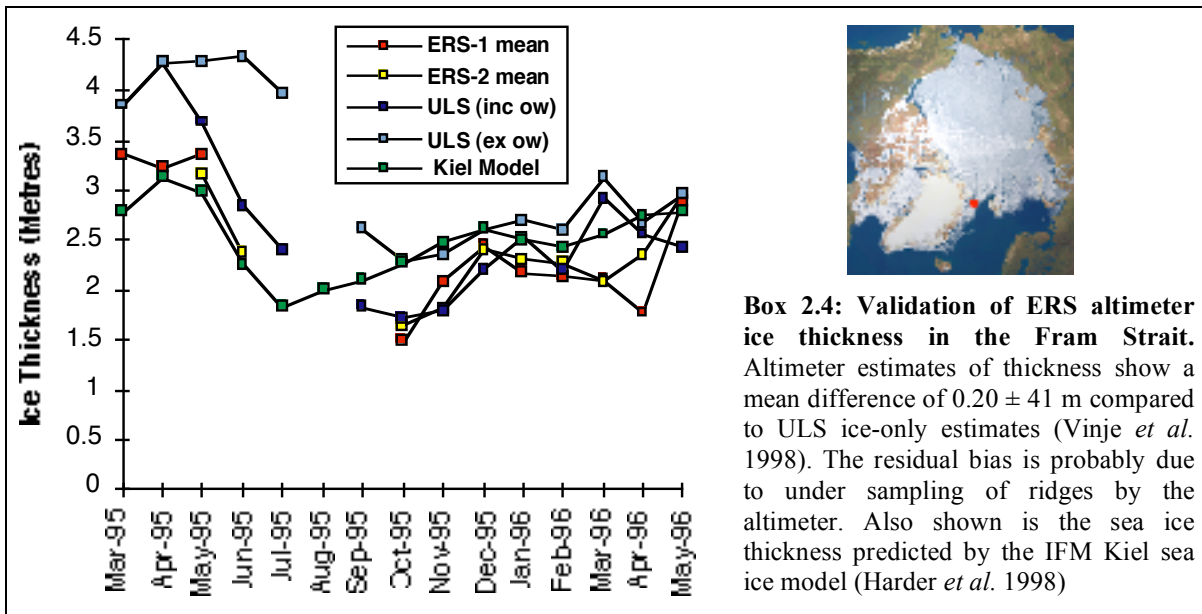
On the other hand, sea ice extent and concentration (*i.e.* percentage coverage of the water surface) has been easily and continuously observed by passive microwave sensors on satellites from 1973 (Gloersen 1992). It was through these measurements that the Weddell Sea Polynya of 1973 - 1976 was discovered, (and the enormous heat losses from the ocean that may occur as a result (Gordon & Comiso 1988)). These measurements also provided the first evidence that Arctic sea ice cover as a whole may be shrinking (Johannessen *et al.* 1995). Sea ice velocity, previously known only from drifting buoy measurements, has been determined through repeated passive microwave observations and with greater resolution with repeated synthetic aperture radar (SAR) measurements.





The importance of sea ice mass flux and the difficulties of direct measurement have led to efforts to assimilate these more-or-less easily observed features of sea ice in models (*e.g.* Thomas *et al.* 1996). As we have noted, however, sea ice is sensitive to errors in the time-averaged atmospheric and oceanic heat fluxes. Data assimilation, largely dependent on satellite-derived ice extents, is susceptible to errors in the forecast heat fluxes. It is recognised (*e.g.* WCRP 1992) that sea ice thickness is potentially the most useful data to assimilate into forecasts of ice mass flux.

Freeboard measurement by satellite (Boxes 2.3 and 2.4) is the only technique to measure sea ice thickness at the time and length scales that investigations of the Earth's climate demands. At present these observations are limited by the resolution of the ERS altimeters; a situation that will continue with ENVISAT. A clear distinction of the ice is possible with an average of only 5 % of the observations, because of the poor resolution of the altimeter. A higher resolution altimeter, the payload of CryoSat, is needed to fully sample of the sea ice.



## 2.4.2 Ice Sheet, Ice Caps and Glacier Mass Imbalance.

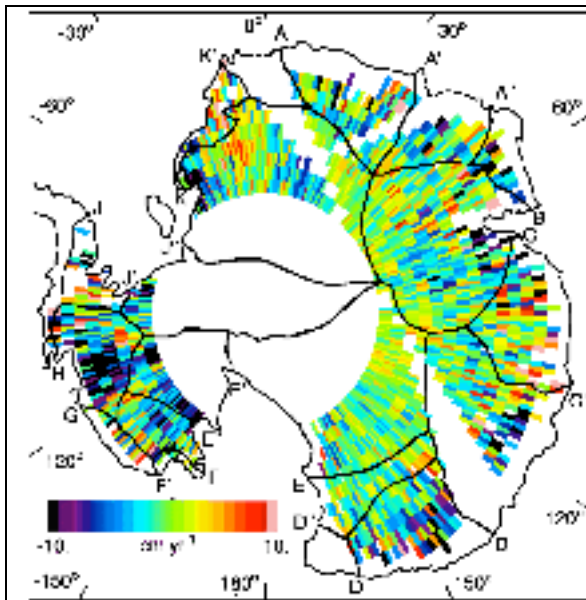
The mass imbalances of the Earth's ice sheets and glaciers are the largest uncertainties in sources of 20<sup>th</sup> century sea level rise and are also a large source of uncertainty in predicting 21<sup>st</sup> century sea level rise (§ 1.1.2 and § 1.2.2). Understanding the present rise and narrowing the uncertainty in future prediction depends on improving knowledge of these imbalances. The difficulty arises because small relative changes in ice mass can effect large changes in sea level in comparison with the observed and predicted rises.

Ground measurement of the imbalances of the Greenland and Antarctic Ice Sheets account for the snow accumulated at the surface and ice lost through surface ablation and ice flow over a grounding line (the line at which ice begins to float). This is difficult to do accurately, partly because the grounding line fluxes are not well-known around the entire coastline. In the main, however, the error arises because the snow fall variability is difficult to sample properly. Glaciological estimates of Antarctic Ice Sheet mass imbalance (*e.g.* Bentley & Giovinetto 1991, Jacobs *et al.* 1992) vary from  $-500 \text{ Gt yr}^{-1}$  to  $+500 \text{ Gt yr}^{-1}$  ( $1.4 \text{ mm yr}^{-1}$  to  $-1.4 \text{ mm yr}^{-1}$  of sea level); that of Greenland between  $-130$  and  $+130 \text{ Gt yr}^{-1}$  (Reeh 1985)

The estimated contribution of  $0.4 \text{ mm yr}^{-1}$  to 20<sup>th</sup> century sea level change of ice caps and glaciers is equal to 8% of their mass. This is a substantial change. Only a small fraction of the Earth's glaciers and ice caps have their mass balance monitored. A global estimate extrapolates these estimates. Typically (*e.g.* Meier 1984) a correlation between observed surface balance, known for some glaciers, and *e.g.* snow accumulation, estimated more-or-less everywhere, is used to extrapolate the observations. There are two problems with this approach. Firstly, the correlation is often poor (*e.g.* Walters & Meier 1989). Secondly, the method ignores the calving flux. This is significant for many of the larger ice caps and





glaciers in the Arctic and may bear no relation to surface balance. In short, this estimate should be treated only with considerable caution. A greatly improved observational base is required.



**Box 2.5: The change in elevation of the Antarctic Ice Sheet** from 1992 to 1996 measured by the ERS-1 and ERS-2 altimeters (from Wingham *et al.* 1998). The data cover 63% of the grounded ice area. The mass imbalance this century is  $60 \pm 70$  Gt yr<sup>-1</sup> or  $\sim 0.3 \pm 0.4$  mm yr<sup>-1</sup> of eustatic sea level. Previous estimates of the grounded ice imbalance vary between -1.4 and +1.4 mm yr<sup>-1</sup> of sea level rise. While demonstrating the great accuracy satellite altimetry provides, 17% of the Ice Sheet margins, (an area larger than the entire Greenland Ice Sheet), and 20% of the interior - together some 33% of the total land cryosphere - remain out of reach of the pulse-limited, ERS or ENVISAT radar altimeters. A principal object of CryoSat is to complete this coverage.

Satellites provide the only feasible method to determine the mass imbalance of the land ice fields in a timely fashion. The first attempt using the Seasat and Geosat altimeters (Zwally *et al.* 1989) predated the era of centimetre orbit accuracy and the reported elevation change has been questioned (Van der Veen 1993, Davis *et al.* 1998). The ERS satellites were the first to provide coverage of Antarctica and Greenland with centimetre orbit precision. In consequence, 63% of the Antarctic Ice Sheet (Box 2.5) is now known to be within 90 Gt yr<sup>-1</sup> ( $\sim 0.25$  mm yr<sup>-1</sup> of global sea level rise) of mass balance. These measurements are being extended to the Greenland Ice Sheet, and will be extended in time with the ENVISAT altimeter.

The ERS and ENVISAT altimeters are designed for the low curvature surface of the ocean. The interior of the ice sheets also have low gradients, typically  $< 0.5^\circ$ . Ice sheet margins, ice caps and glaciers have higher gradients. ERS-ENVISAT altimetry is unable to provide accurate trends in these regions (Box 2.5). The ice sheet margins are exposed to atmosphere and ocean forcing, are the most dynamic parts of the ice sheets (Alley & Whillans 1991), and may be undergoing change (e.g. Basin G-H in Box 2.5 is decreasing in elevation rapidly). There are no observations of 17% of the Antarctic margins. This may appear a small proportion, but it accounts for 16% of the entire land cryosphere, more than the entire Greenland Ice Sheet. A proportional loss occurs over Greenland. There is no coverage of the world's ice caps and glaciers. Providing this coverage is a goal of CryoSat.

		Issue: 1 Date: 21. September 1999 Page: 13
---	--	--

## 2.5 The Contribution to Earth Explorer and other International Programs.

The CryoSat mission will take place in the context of other experiments aimed at understanding the cryosphere. In this section we highlight activities which together with CryoSat enable a more complete approach to the science uncertainties outlined in § 2.2. These activities include other components of the ESA Explorer Program (§ 2.5.1), other ESA missions (§ 2.5.2), other non-ESA missions, particularly the US GRACE and ICESAT missions (§ 2.5.3) and (§ 2.5.4) the observation programs such as CLIVAR and ACSYS organised under the umbrella of the World Climate Research Program (WCRP) and International Geosphere-Biosphere Program (IGBP).

### 2.5.1 Relevance to ESA Earth Explorer Objectives.

The Science and Research Element (ESA 1998) of the Earth Explorer Program is a broad program attacking scientific uncertainties across the physics and chemistry of the solid and fluid Earth and across the range of diurnal to centennial time scales. It also addresses the impacts of global change on natural variability and human activity. Within this spectrum, the cryosphere is an essential component. It is part of the land and ocean surface, with a significant impact on the radiation balance of the atmosphere. It is an integral part of the physical climate, Theme 2 of the Science and Research Element.



The task of the Explorer Program is to use satellites to provide data to stimulate and verify integration of numerical models of the Earth system. Measurements of sea and land ice are key components of the Medium and Long Term Component of Theme 2, and these measurements fall squarely within the objectives of the Earth Explorer Program (ESA 1988). The “Topography” mission (ESA 1996) was one of nine missions identified by ESA as providing important deliverables of the Explorer Program. The cryospheric deliverables were principal deliverables of the “Topography” mission: CryoSat will provide key deliverables of the Explorer Program.

### 2.5.2 Complementarity with ERS, ENVISAT and Earth Explorer Core Missions.

The ERS satellites were the first and only satellites to provide altimetry of Earth’s polar latitudes greater than 72°. The ERS program and European Earth Observation scientists are at the forefront of polar science. Recent achievements include the discovery of major flow features on the Antarctic Ice Sheet (Bamber 1994), the first description of the marine gravity fields of the Arctic and Antarctic Seas (Laxon & McAdoo 1994, McAdoo & Laxon 1997), the first accurate constraints on the mass imbalance of the Antarctic interior (Box 2.5) and the first observation of sea ice thickness from space (Box 2.3). These observations will be continued by ENVISAT from 2000. CryoSat will sustain this European lead by extending the spatial and temporal coverage of these satellites to complete coverage of the fluctuations of sea ice and ice sheets.

The Gravity Field and Steady State Ocean Circulation Explorer (GOCE) Core mission will provide to ~ 84° of latitude the gravity field of the Earth to ~ 100 km scales. The accurate GOCE geoid will provide an important addition to CryoSat observations. The distinction

---

		Issue: 1 Date: 21. September 1999 Page: 14
---	--	--

between ice and ocean surfaces that permits the measurement of sea ice thickness (Box 2.3) have also allowed the first determination of the variability of dynamic topography of Arctic Ocean to 82° N (Peacock 1998). An accurate GOCE geoid together with CryoSat measurements may permit investigations of the mean polar circulation to 86° N. CryoSat will uniquely provide continuous coverage of these latitudes. The use of GOCE gravity and CryoSat elevations over the Antarctic Ice Sheet margins will also provide an estimate of ice sheet thickness and bottom topography. This topography is poorly known and yet is a control on ice sheet stability (Hughes 1981).

Improved understanding of the moderation of the ocean-atmosphere interaction by sea ice will provide important ancillary information to studies of the Earth's radiation budget, and the distribution of precipitation. These are also important processes in the cryosphere. The Explorer Program Core Earth Radiation Mission, and a potential "Precipitation" Mission, will benefit and support the CryoSat mission.

### 2.5.3 Complementarity with Other Missions.

There are three missions of particular complimentary importance to CryoSat. These are the ICESAT, JASON-1 and GRACE missions. The polar regions experience between 50% and 90% cloud cover (Hansen-Bauer 1992). CryoSat will provide complete and continuous coverage of the Earth, but is limited in its resolution. ICESAT may provide details of the sea ice and land ice roughness spectrum, but the limits imposed by cloud cover will seriously reduce sea ice thickness measurements and very seriously reduce change measurements at fixed ice sheet locations (§ 3.1). By selecting a launch date of 2002 (§ 2.5) the optimal combination is achieved through the CryoSat radar altimeter and the US ICESAT.

Sea-level will be monitored by the JASON-1 mission following TOPEX/Poseidon. With time these satellites will provide a greatly improved estimate of sea level rise. The US GRACE mission, with a launch date of 2001, will measure the time-variant gravity field of the Earth to a resolution of ~ 500 km. GRACE may permit the distinction of steric (thermal) and mass changes in altimeter observations of sea level, and provide direct constraints on the theory of post-glacial rebound. It also provides probably the only way constrain the land-ocean water exchange, which introduces perhaps 2 cm century<sup>-1</sup> uncertainty into the sea level rise budget (Chao 1994). The mass imbalance of the Antarctic and Greenland Ice Sheets will also produce changes in gravitational potential. CryoSat observations may allow a separation of present imbalance and post-glacial rebound in the GRACE observations.

There are numerous climate and forecasting missions that will improve knowledge of the cryosphere. These include the ongoing series of sea ice extent; increasing knowledge of sea ice velocity from SAR missions such as ERS, RADARSAT and ENVISAT; and improving atmospheric temperature, wind and precipitation fields provided by forecast models, in part through satellite observations. These will improve capability to determine sea ice fluxes through data assimilation. As observed in § 2.4.1, sea ice thickness data remains of central importance.

#### **2.5.4 Complementarity with Climate Change Programs.**

The objectives of the CryoSat mission are most important to the Climate Variability and Predictability Program (CLIVAR; WCRP 1998), which builds on the World Ocean Circulation Experiment (WOCE), and the Arctic Climate System Study (ACSYS; WCRP 1992). These are components of the World Climate Research Program (WCRP). CryoSat is directly relevant to CLIVAR programs on the Atlantic Thermohaline Circulation, Southern Ocean Climate Variability, and North Atlantic Oscillation program (WCRP 1998). These programs all identify a need for sea ice thickness and mass. The same need is also identified by the ACSYS program (WCRP 1992). To improve the performance of sea ice models and to analyse the variability of sea ice, ACSYS has observational and Modeling projects concerning the role of sea ice in climate. ACSYS and CLIVAR rely heavily on satellites for ice concentration and drift, and on new sensors such as CryoSat for sea ice thickness.

These programs are also concerned to organise oceanographic observations needed to provide a picture of the internal variability of the ocean. WOCE ocean sections run along the boundary of the North Atlantic and the Iceland and Labrador Seas, and through the Greenland Sea. ACSYS intends the systematic occupation of five sections in the Arctic Ocean (ACSYS 1998). As part of its Sea Ice Project, it will also maintain drifting buoys through the International Arctic Buoy Program and ULS thickness data. In the Southern Ocean, CLIVAR intends to maintain three WOCE sections across the Antarctic Circumpolar Current. UK and German institutes intend to add sections to provide the mean circulation and variability of the Weddell Sea “box”, and repeat sections across the Ronne-Filchner Ice Shelf front, as part of the International Antarctic Zone (iAnZone) Program.

### **3 General Mission Characteristics**

The primary science goals of the CryoSat mission are to determine the trends in mass of the Earth’s permanent ice fields. This will be achieved by measuring their change in thickness. In this section, the accuracy with which these mass trends are required by science is translated into requirements on the measurement of thickness. This requires some discussion of the natural fluctuations of sea ice and land ice thickness, together with a consideration of their spatial distribution over the Earth.

#### **3.1 Scientific Objectives of the CryoSat Mission**

##### **3.1.1 Primary and Secondary Mission Goals.**

The purpose of the CryoSat mission is to determine trends in the ice masses of the Earth. Of principal importance is to (a) test the prediction of thinning perennial Arctic sea ice due to global warming, and (b) reduce uncertainty in the contribution to sea level of the Antarctic and Greenland Ice Sheets. These questions provide the primary mission goals. CryoSat will provide observations for:

- The determination of regional and basin-scale trends in perennial Arctic sea ice thickness and mass.
- The determination of regional and total contributions to global sea level of the Antarctic and Greenland Ice Sheets.

Trends determined by CryoSat within its lifetime will be limited by the natural variability of ice thickness. The importance of its measurements will be increased by a future flight of an equivalent mission two decades or so later. Nonetheless, the actual performance (Box 3.1) will allow CryoSat in its own lifetime to determine whether the observed changes in sea ice (§ 2.4.1) signal important trends in Arctic climate or merely the ephemera of interannual variability at short spatial scales, and to reduce the uncertainty in the ice sheet contribution to sea level to a magnitude similar to that associated with other sources of sea level rise.

The secondary mission goals of CryoSat are to make observations of:

- The seasonal cycle and interannual variability of Arctic and Antarctic sea ice mass and thickness;
- The variation in thickness of the world's ice caps and glaciers.

These surfaces are not CryoSat design drivers. Nonetheless, CryoSat will make extensive measurements of seasonal sea ice fields. In addition, CryoSat has a swath capability (§ 3.1.2). It will provide measurements over ice caps and glaciers which are scientifically important. The CryoSat coverage (§ 3.4.6), data-rate and ground segment will accommodate these measurements.

### 3.1.2 Overview of Science and Measurement Requirements.

The CryoSat mission will determine trends in ice mass through repeated measurements of ice thickness. A residual uncertainty in the mass and thickness trends of sea and land ice will remain at the end of the mission. The scientific requirements of the mission specify this residual uncertainty. It should be recognised at the outset that this uncertainty cannot be smaller than the natural variability in thickness. There is limited value in making observations with greater precision than the natural lower limit. The determination of requirements is thus a two-stage process. The first task (§ 3.3) is to characterise the natural variability of thickness. The second task (§ 3.4) is to determine the measurement accuracy that makes the residual uncertainty close to the natural variability. This is the *required* measurement accuracy. These considerations will lead us to the science and measurement requirements in Table 3.1.

We use the symbol  $\eta$  to describe a variability of a mass rate, quoted typically in units of  $\text{Gt yr}^{-1}$ . This is useful to compare a mass variation with sea level rise (1 mm  $\text{yr}^{-1}$  eustatic sea level equals 360  $\text{Gt yr}^{-1}$  of water). We use the symbol  $\sigma$  to describe the variability of a mass rate per unit area. This is a more convenient quantity to compare with a change in thickness, and for this reason we use units of cm of ice mass  $\text{yr}^{-1}$ , assuming a density of  $915 \text{ kg m}^{-3}$ , written  $\text{cm yr}^{-1}$  ice equivalent (i.e.).

---

In general a good deal the variability of ice mass occurs at short spatial scales, and the variability of mass is a strong function of the area under consideration. We use the symbol  $\bar{\sigma} = \eta / A$  to characterise the mass variability of an extensive area  $A$  as a thickness variability. If the mass variation is perfectly correlated over an area  $A$ , then  $\bar{\sigma} = \sigma$  but this is generally not the case. Typically  $\bar{\sigma}$  will be considerably smaller than  $\sigma$  for areas in excess of  $10^4 \text{ km}^2$ .

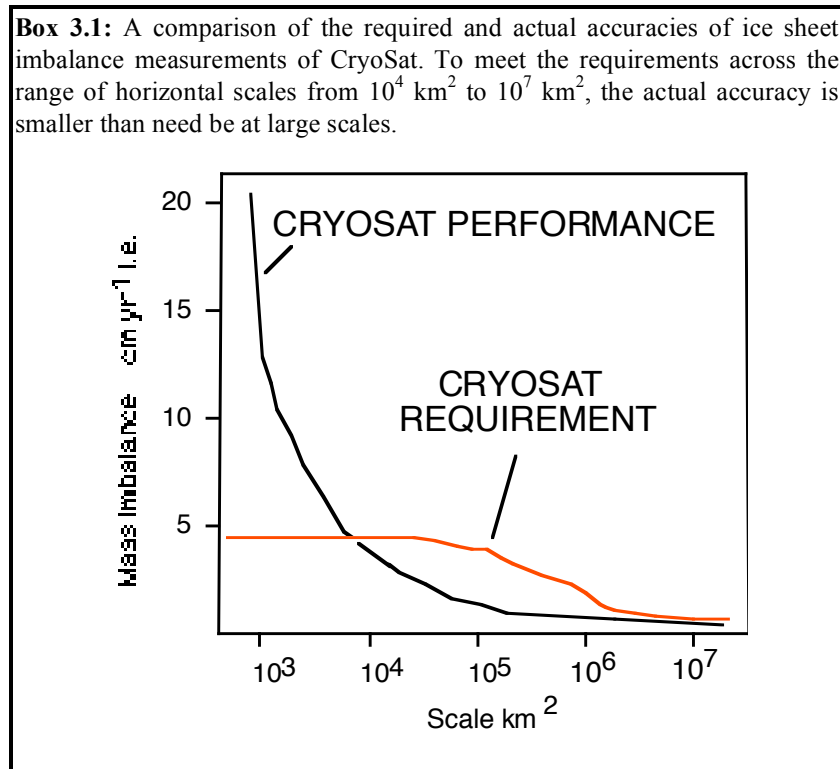
The scientific requirements specify the residual uncertainty  $\bar{\sigma}_r$  in trends at the end of the mission. The lowest bound of the residual uncertainty is the natural variability  $\bar{\sigma}_n$ . Measurement error  $\bar{\sigma}_m$  will increase residual uncertainty according to

$$\bar{\sigma}_r^2 = \bar{\sigma}_n^2 + \bar{\sigma}_m^2 \quad (3.1.1)$$

We determine the residual uncertainty by requiring it to be close to the natural lower bound, and we give *close* a quantitative expression by requiring that the observations increase by no more than 10% the residual uncertainty in a trend due to natural variability, that is,

$$\bar{\sigma}_r = 1.1\bar{\sigma}_n \quad (3.1.2)$$

The behaviour of the natural variability is the subject of § 3.3. The variation of  $\bar{\sigma}_r$  that results for ice sheets is illustrated in Box 3.1 as a function of spatial scale.



The measurement requirements are then determined by substituting (3.1.1) into (3.1.2) to obtain



$$\bar{\sigma}_m \sim 0.5\bar{\sigma}_n \quad (3.1.3)$$

It is not practical with a single satellite to satisfy (3.1.3) at all of the spatial scales illustrated in Box 3.1. The actual measurement error will become large at small spatial scales, as the figure shows. Therefore we demand that eqn. (3.1.3) is satisfied over a narrower range of scales. In the case of sea ice, we argued in § 2.3 that  $10^5 \text{ km}^2$  is the lowest scale at which trends may become visible. We accordingly require eqn. (3.1.2) satisfied at  $10^5 \text{ km}^2$ . In the case of the ice sheets, there are important scientific questions at regional scales and large scales (§ 2.2.2). Therefore we require eqn. (3.4.2) satisfied at  $10^4 \text{ km}^2$  *and* at  $13.8 \times 10^6 \text{ km}^2$ . The latter area is the total area of the Ice Sheets. This leads to the requirements shown in Table 3.1.

**Table 3.1:** The CryoSat Science and Measurement Requirements.

Requirement	Arctic Sea Ice $10^5 \text{ km}^2$	Ice Sheets $10^4 \text{ km}^2$	Ice Sheets $13.8 \times 10^6 \text{ km}^2$
$\bar{\sigma}_r(\eta_r)$	3.5 cm yr <sup>-1</sup> i.e.	8.3 cm yr <sup>-1</sup> i.e.	1 cm yr <sup>-1</sup> i.e. (130 Gt yr <sup>-1</sup> )
$\bar{\sigma}_m$	1.6 cm yr <sup>-1</sup>	3.3 cm yr <sup>-1</sup>	0.7 cm yr <sup>-1</sup>

### 3.2 The Measurement of Thickness and Mass Variations.

Variations in the thickness of ice at the surface of the Earth give rise to changes in the shape of the Earth. If changes in the shape of Earth's ice covered surfaces are measured, the change in thickness of the ice can be determined. Combined with knowledge of the density of ice, changes in the mass of ice may also be measured. In a satellite measurement, changes in the Earth's shape are made using radar or laser ranging from a satellite whose position is determined within a reference frame, the ellipsoid, whose origin is the Earth's centre of mass<sup>4</sup>. If the satellite is a height  $h_s$  above the ellipsoid, and the electromagnetic wave takes a time  $\tau$  to travel with a velocity  $v$  to the surface and back, the elevation or height  $h$  of the surface with respect to the ellipsoid is

$$h = h_s - \frac{v\tau}{2} \quad (3.2.1)$$

Variations in height  $\Delta h$  measured through repeated observations of  $h$  are the change with respect to the ellipsoid. In the case of the land ice, the total change is that due to the vertical motion of the solid Earth and the ice thickness change. In general, the the vertical motion of the Earth is small in comparison with the uncertainties of thickness change (Wahr 1994), and observed changes with respect to the ellipsoid are to first order changes in ice thickness. (We are not here concerned with the measurement of land ice thickness itself). Variations in land ice mass per unit area  $\Delta m_i$  are determined through

$$\Delta m_i = \rho_i \Delta h \quad (3.2.2)$$

where  $\rho_i$  is the density of land ice. The actual density of land ice varies in depth and time, so that the density  $\rho_i$  is an *effective* density.

---

<sup>4</sup> Errors arising from uncertainties in the location of the ellipsoid with respect to the solid Earth are very small in the context of ice thickness changes and will be ignored.

---

Satellites observe the shape of the Earth discretely. In a time interval  $\Delta s$  centered at  $s_i$ , they observe the set of heights  $h(s_i, \mathbf{x}_{ji})$  over an area. In principle, one may attempt to determine the change in thickness  $\Delta \bar{h}$  over an area using

$$\Delta \bar{h}(s_2 - s_1) \sim \sum_j W(\mathbf{x}_{j2}) h(s_2, \mathbf{x}_{j2}) - W(\mathbf{x}_{j1}) h(s_1, \mathbf{x}_{j1}) \quad (3.2.3)$$

where  $W$  is an interpolation function. Speaking practically, eqn. (3.2.3) describes taking the difference between two digital elevation models. The difficulty with this approach is that spatial locations at times  $s_1$  and  $s_2$  are generally not the same. The interpolation errors are not time invariant. Experience has shown that over ice sheets, this error may be large for single-satellite spatial- and temporal- sampling. The error may be removed by ensuring that  $\mathbf{x}_{ji} = \mathbf{x}_{jk}$  for all times  $s_i$ . This can be arranged using observations at crossing points of the satellite orbit. Eqn. (3.2.3) is then replaced with

$$\Delta \bar{h}(s_2 - s_1) \sim \sum_j W(\mathbf{x}_j) \Delta h(s_2 - s_1, \mathbf{x}_j) \quad (3.2.4)$$

The interpolation errors are those associated with interpolating  $\Delta h$  and not  $h$ . Typically, these errors will be two orders of magnitude smaller.

Sea ice is floating on an ocean surface which is varying with respect to the ellipsoid due to tides and changes in ocean dynamics. Measuring sea ice thickness requires the simultaneous measurement of the change in height of the ocean surface with respect to the ellipsoid. Sea ice thickness is determined from the difference of the two measurements, or sea ice *freeboard*  $f$ . Because the ice of effective density  $\rho_{si}$  is floating in sea water of density  $\rho_w$ , its total thickness is given by

$$t = f \left( \frac{\rho_w}{\rho_w - \rho_{si}} \right) \quad (3.2.5)$$

Sea ice mass per unit area  $m_{si}$  is determined through

$$m_{si} = \rho_{si} t \quad (3.2.6)$$

Along-track elevations are separated using the backscatter coefficient (Box 2.3) into ocean and ice,  $x = x_j$  and  $x = x_i$  respectively, or rejected as ambiguous. A smoothed sea-surface elevation is formed from the ocean elevations. The freeboard at the ice locations is then determined as an anomaly (Box 2.3) from the smoothed sea-surface elevation:

$$f(x_i) = h(x_i) - \sum_j W_i(x_i, x_j) h(x_j) \quad (3.2.7)$$

Areal estimates of thickness are then formed using eqns. (3.2.5) and (3.2.6), and variations in thickness  $\Delta t$  or mass  $\Delta m_{si}$  using interpolations of the form eqn. (3.2.3).



### 3.3 Natural Variability in Ice Mass and Density and Atmospheric Refraction

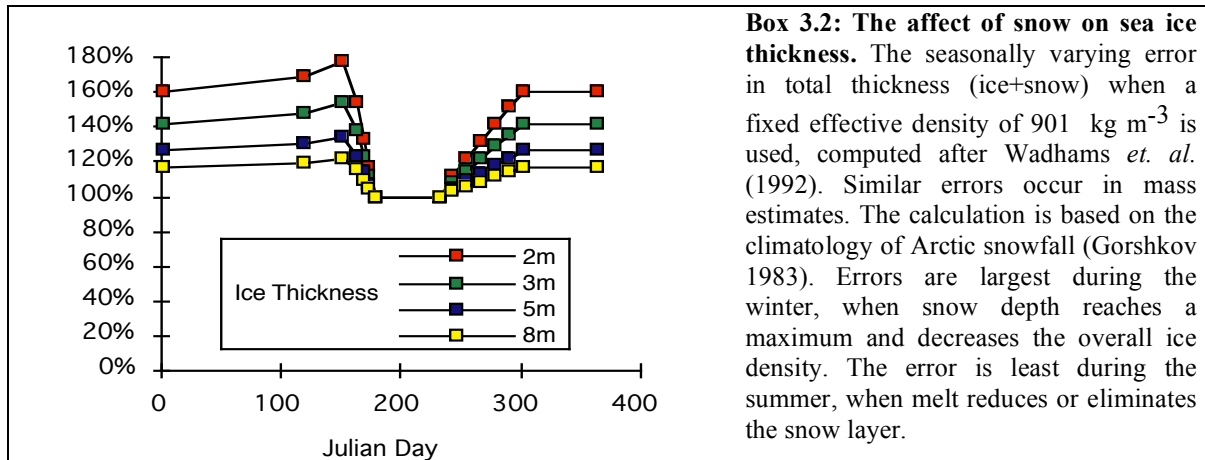
In this section we describe uncertainties introduced by the natural variability in ice and snow mass and density. These parameters will not be measured by CryoSat for reasons of cost or practicality. These uncertainties generate *a-priori* lower bounds on the reduction in uncertainty CryoSat may achieve. The natural variability in mass and density affect sea ice (§ 3.3.1) and land ice (§ 3.3.2) measurements differently.

#### 3.3.1 Sea Ice Mass Variability.

The natural variability  $\delta f$  in sea ice freeboard arises through fluctuations  $\delta m$  in ice mass and  $\delta \rho_{si}$  in effective density. Using eqns. (3.2.5) and (3.2.6) one has

$$\delta f = \delta m \frac{\rho_w - \rho_{si}}{\rho_w \rho_{si}} + \delta \rho_{si} \frac{m}{\rho_{si}^2} \quad (3.3.1)$$

In the case of sea ice at large-scales, there is little idea of the natural variability of  $\delta m$ . The interannual variation in summer thickness of Arctic sea ice of  $\sim 25 \text{ cm yr}^{-1}$  (Box 2.2) is close to that produced by the interannual variations  $\delta \rho_{si}$  in summer effective density and on this basis one may argue that interannual mass fluctuations are small. Noting that a *smaller* natural variability implies a *tighter* measurement requirement, we make this assumption.

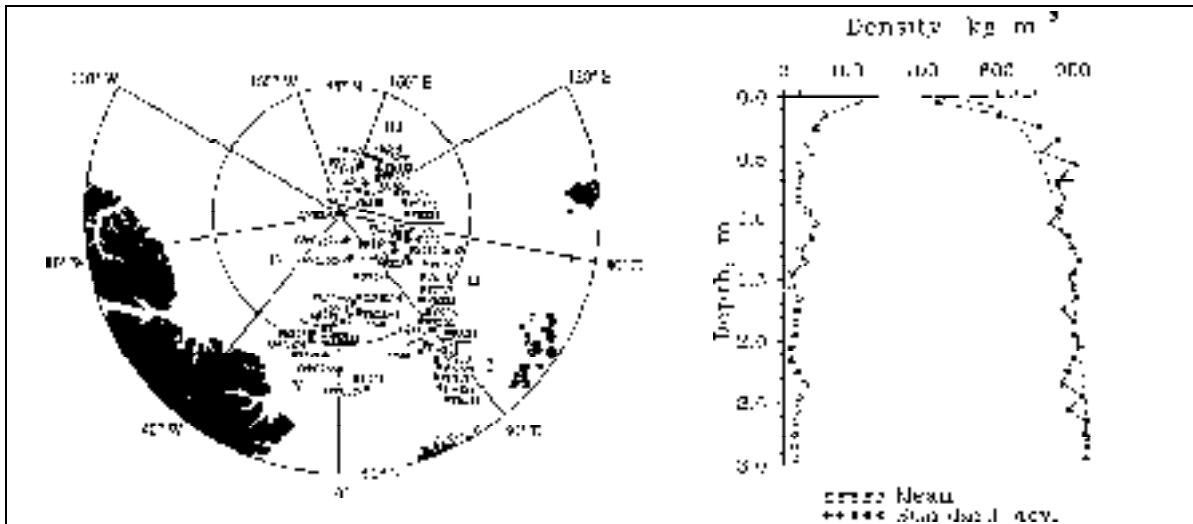


The situation is quite different for seasonal variations in mass. The effective density<sup>5</sup>  $\rho_{si}$  that appears in eqns. (3.2.5) and (3.2.6) is the average density of a column through the sea ice. Sea ice is comprised of frozen sea water and snow precipitated on the surface. Variations in accumulated snow will give rise to variations in the effective density. Because

<sup>5</sup> Experiments usually measure the draft-to-freeboard ratio. Values of 7.89 (Wadhams 1992) and 7.35 (Vinje *et al.* 1998) can be found in the literature. With a density of sea water equal to  $1024 \text{ kg m}^{-3}$ , the effective densities of sea ice are respectively  $908 \text{ kg m}^{-3}$  and  $901 \text{ kg m}^{-3}$ . On the other hand, Eiken *et al.* (1995) give  $889 \text{ kg m}^{-3}$  for the effective density of summer ice in the Arctic. For definiteness, we take the effective density  $901 \text{ kg m}^{-3}$ . The variation we assume in summer effective density accomodates these differences. Variations in sea water density are order 0.1%. We ignore these here.

these variations are generally unknown, errors are introduced into measurements of thickness and mass (Box 3.2).

The error due to snow mass will be a maximum at the end of the winter accumulation, and negligible at the end of the melting season. On the other hand, once meltwater appears on the surface of the ice, the distinction between the backscattering coefficient of ice and water greatly reduces. For this reason, estimates of a trend in ice thickness will be made with the onset of freezing. The uncertainty is then that due to the variability in effective ice density at the end of the summer (Box 3.3). We shall term this uncertainty  $\varepsilon_t$ .



**Box 3.3: Ice density at the completion of the melt season.** During August and September 1991 sea ice properties were measured over a large fraction of the Arctic Ocean (Eicken *et al.*, 1995). At stations marked OP (left hand panel) ice density was measured as a function of depth. The mean (right hand panel, right hand graph) and standard deviation (right hand panel, left hand graph) of density as a function of depth were determined. Overall, ice density was measured as  $887 \pm 20 \text{ kg m}^{-3}$ . For an ice thickness of 3 metres, the corresponding uncertainty in thickness is  $\pm 40 \text{ cm}$ .

If the mission duration is  $N$  (integer) years, there will be  $N$  observations of the thickness, and the natural variability of the trend will equal the standard deviation of the gradient of a straight line drawn through  $N$  points, each with a variability  $\varepsilon_t$ . The variability will appear in the freeboard measurement (eqn. 3.2.5) with approximately one eighth of the amplitude. The lower bound placed by natural variability of sea ice freeboard trends is

$$\bar{\sigma}_n = \frac{\varepsilon_t}{8} \sqrt{\frac{12}{N(N-1)(N+1)}} \times \left( \frac{1}{1 \text{ year}} \right) \quad (3.3.3)$$

From Box 3.3, the value of  $\varepsilon_t$  is  $\sim 40 \text{ cm}$ .

### 3.3.2 Land Ice Mass Variability

Variations in snow fall give rise to variability in mass imbalance. The variation in snowfall occurs at a density of  $\sim 400 \text{ kg m}^{-3}$ . This amplifies its appearance in the thickness variation

in comparison with those due to ice flow. The matter is complicated by the fact that as snowfall varies at the surface, the firn column beneath, densifying under its own weight, experiences a fluctuating overburden. In consequence the firn column density also fluctuates (Wingham 1999). The thickness variation due to snowfall is inseparable from that due to the fluctuating density of the firn column. The two must be dealt with simultaneously.

For ice sheets the interannual snowfall variability is usually expressed as a fraction  $\alpha$  of the mean annual accumulation rate  $\dot{M}$ . When dry firn, densifying under its own weight, experiences fluctuations in snowfall, the uncertainty  $\sigma_n$  in a thickness change measurement varies with observation interval  $T$  (in years) according to

$$\sigma_n = r(T) \left( \frac{1}{T^{1/2}} \right)^{1/2} \alpha \dot{M} \quad (3.3.4)$$

where  $r(T)$  arises from the densification (Wingham 1998). In eqn. (3.3.4) the '1' is 1 year and has dimensions of time. It has limiting forms

$$r(T) = \begin{cases} \rho_{snow} / \rho_{ice} & T \sim 1 \text{ year} \\ 1 & T \sim 100 \text{ years} \end{cases} \quad (3.3.5)$$

For short intervals the fluctuations appear with the density of snow  $\rho_{snow}$ ; for long intervals they occur with the density of glacier ice  $\rho_{ice}$ . The statistics of snowfall variations are reasonably established from ice core data (*e.g.* Van der Veen 1993, Wingham *et al.* 1998). For Greenland,  $\alpha \sim 0.55$ ; for Antarctica  $\alpha \sim 0.34$ . For CryoSat observation intervals one has

$$\sigma_n \sim \begin{cases} 0.8 \dot{M} / T^{1/2} & \text{Antarctica} \\ 1.3 \dot{M} / T^{1/2} & \text{Greenland} \end{cases} \quad (3.3.6)$$

If temperature is significant in aiding densification  $r(T)$  approaches the lower limit in eqn. (3.3.5) more rapidly and eqn. (3.3.6) overestimates somewhat the variability.

(3.3.6) describes the fluctuations at a point. Snowfall over ice sheets decorrelates over large distances (Enomoto 1991). The decorrelation length is  $\sim 200$  km (Wingham *et al.* 1998 and references therein). The variability  $\bar{\sigma}_n$  a region of area  $A$  (in  $\text{km}^2$ ) which is larger than the area over which snowfall is correlated is then

$$\bar{\sigma}_n \sim \begin{cases} 160 \sqrt{\pi / A} \dot{M} / T^{1/2} & \text{Antarctica} \\ 260 \sqrt{\pi / A} \dot{M} / T^{1/2} & \text{Greenland} \end{cases} \quad (3.3.7)$$

Eqn (3.3.7) sets the lower bound for measurements of a land ice thickness trend.

### 3.4 The Measurement Requirements

#### 3.4.1 Coverage, Mission Duration and Measurement Accuracy.

We assume that CryoSat will have a mission duration  $T$  of 3 years. For sea ice, the natural variability  $\bar{\sigma}_n$  is 3.1 cm yr<sup>-1</sup> from eqns. (3.1.3). This gives a value of 1.6 cm yr<sup>-1</sup> for  $\bar{\sigma}_m$  on using eqn. (3.1.3).

For land ice, the situation is more complicated. The natural variability given by eqn. (3.3.7) depends on accumulation rate, which is spatially variable. The science requirement of eqn. (3.1.3) at 10<sup>4</sup> km<sup>2</sup> leads to a spatially varying measurement accuracy, according to whether the mean accumulation rate is high or low. The largest uncertainty in connection with Ice Sheets, however is that of the Antarctic margins. We therefore take the average accumulation rate of this region, 15.7 cm yr<sup>-1</sup> (Table 3.2), in satisfying this requirement. 10<sup>4</sup> km<sup>2</sup> is less than the correlation distance of snow accumulation. The natural variability  $\bar{\sigma}_n$  equals  $\sigma_n$  in this case, and eqn. (3.3.6) provides the variability due to snowfall. Its value is 7.25 cm yr<sup>-1</sup>. This gives a measurement error  $\bar{\sigma}_m$  of 3.62 cm yr<sup>-1</sup>.

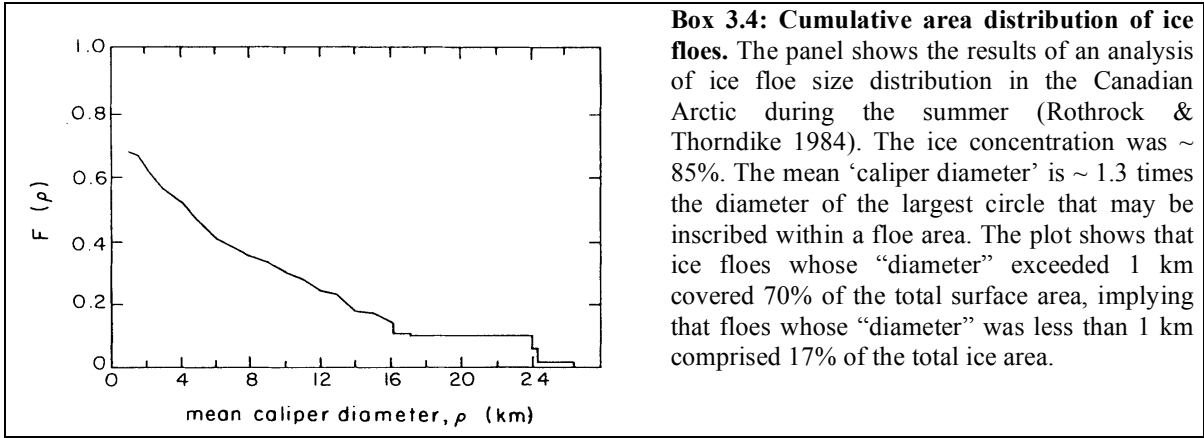
To deal with the ice sheets at large scales, one does need to take account of the fact that the accumulation varies spatially. For the ice sheet requirement at 13.8 x 10<sup>6</sup> km<sup>2</sup> we distinguish between the “interior” and “exterior” regions of the ice sheets in which accumulation is usually higher. Table 3.2 then gives the natural variability of total ice sheet mass as 145 Gt yr<sup>-1</sup>. The resulting measurement requirement is  $\eta_m$  equal to 73 Gt yr<sup>-1</sup> from eqn. (3.4.3), or, equivalently,  $\bar{\sigma}_m$  equal to 0.5 cm yr<sup>-1</sup>.

**Table 3.2:** 3-year Snowfall Variability of the Ice Sheets.

	Area $A$ km <sup>2</sup> x 10 <sup>6</sup>	Accumulation cm yr <sup>-1</sup> i.e.	$\bar{\sigma}_n$ cm yr <sup>-1</sup> i.e.	$\eta_m$ Gt yr <sup>-1</sup>
Antarctic “Interior”	7.7	13.4	0.8	55.8
Antarctic “Exterior”	4.4	15.7	1.2	46.2
Greenland “Interior”	1.2	28.7	3.3	76.0
Greenland “Exterior”	0.5	53.7	24.5	101.1
Total	13.8		1.1	145

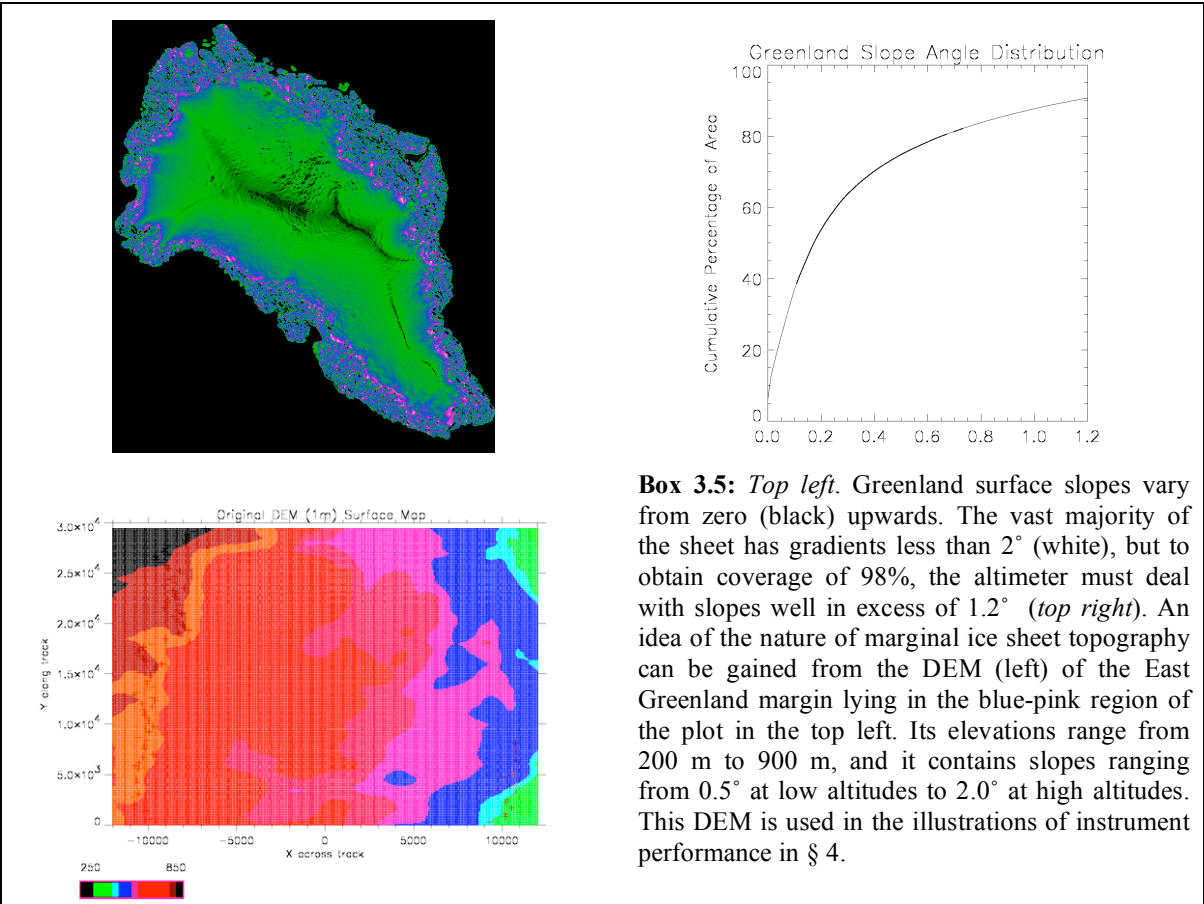
i.e. = ice equivalent thickness



The mission requirements  $\bar{\sigma}_r$  that arise from these data have been given already in Table 3.1.



### 3.4.2 Horizontal Resolution.

Over sea ice the horizontal resolution needs to distinguish ocean and sea ice surfaces whose simultaneous height is required for the measurement (§ 2.2). This distinction is based on the differing backscatter coefficient of the ice and the ocean (Box 2.3).



		Issue: 1 Date: 21. September 1999 Page: 25
---	--	--

When sea ice floes, or the leads lying between them, are smaller than the sensor resolution, the two surfaces may not be distinguished. Thus, the resolution determines the proportion of sea ice floe area that may be sampled. Floe and lead size varies with time of year and with region. There are few quantitative studies of the relation of floe area to total area coverage. What evidence there is (Box 3.4), suggests that 80% of Arctic floes in summer have dimensions larger than 1 km. We require 1 km resolution over sea ice.

Over land ice, the need for horizontal resolution arises from the science requirement (§ 3.4.1) to provide coverage of the Antarctic and Greenland Ice Sheets. This demands coverage of surface gradients up to  $2^\circ$  (Box 3.5). Accurate change measurements with pulse-limited altimeters such as the ERS and ENVISAT altimeters become difficult when the surface gradients exceed the angular width of the altimeter beam,  $\sim 0.5^\circ$ . Some 17% of Antarctica and 23% of the Greenland Ice Sheet exceed this gradient (Box 3.5). We require sufficient horizontal resolution to meet the vertical accuracy requirement over the marginal regions of the Antarctic and Greenland Ice Sheets.

#### 3.4.3. Spatial and Temporal Sampling.

The science requirements for sea ice demand sampling at  $10^5 \text{ km}^2$  ( $\sim 300 \text{ km}$  by  $300 \text{ km}$ ). The effect of snowfall variability (§3.3.1) makes it necessary that the primary mission goal measurements of sea ice fall within 1 month in any one year. This places an upper bound on the temporal sampling. This sampling is also suitable for the secondary sea ice objectives.

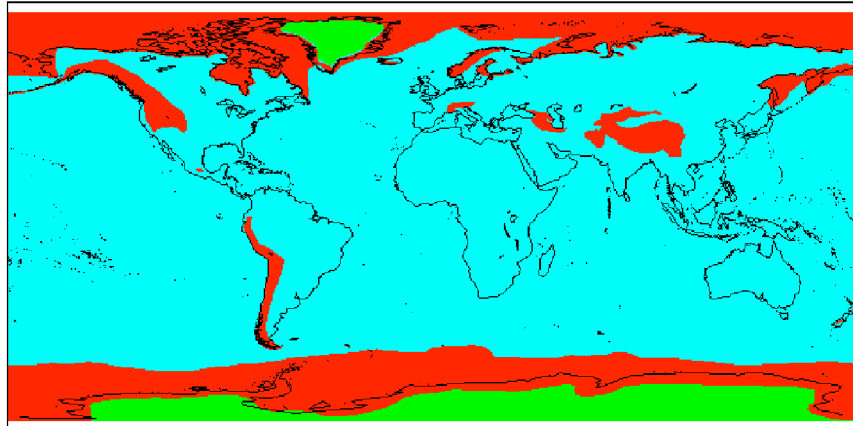
For land ice, the requirements is spatial sampling at  $10^4 \text{ km}^2$  ( $\sim 100 \text{ km}$  by  $100 \text{ km}$ ). There is no specific temporal sampling requirement, although the accuracy of the trend estimation (§ 4.3.3) depends on the number of temporal samples. To maximise coverage over ice caps and glaciers, dense spatial sampling consistent the primary mission goal temporal sampling should be achieved.

The spatial pattern of samples need not repeat, provided it retains a constant temporal and spatial sampling density. Sea ice is a moving mass field. Were the sample pattern to repeat itself, measurements would still observe different ice. Changes in the orbit pattern are accommodated by the interpolation function  $W$  in eqn. (3.2.3). The land ice measurement uses crossovers of the orbit (§ 3.2), and in doing so removes the effect of the topography. Changes in the pattern of cross-overs are accommodated with the function  $W$  in eqn. (3.2.4). (This has been demonstrated using Antarctic data from the drifting 37-day subcycle of the ERS-1, geodetic mission phase (Arthern 1996)).

#### 3.4.4 Spatial Extent.

The spatial extent (Box 3.6) is determined by the secondary mission goals.





**Box 3.6:** CryoSat spatial extent is determined by the distribution of marine and land ice. In the Northern Hemisphere, sea ice at its maximum extent covers the Arctic Ocean, Bering Strait, Kara Sea, Hudson Bay and Greenland and Norwegian Seas and extends in a down the east coast of North America to latitudes of  $45^\circ$ . In the Southern Hemisphere, the ice extends from the Antarctic continent to a winter maximum  $\sim 50^\circ$  latitude. The land ice covers the Antarctic and Greenland Ice Sheets, the Russian, Norwegian, Canadian and Alaskan Arctic, and glaciers of the world widely scattered over the continents, including the Himalayas, the Rocky Mountains, Andes, European Alps and New Zealand Southern Alps. The red regions of the plot show where high resolution altimetry is required and green regions where pulse-limited altimetry is sufficient. The area of the high resolution mask is  $\sim 59 \times 10^6 \text{ km}^2$ , or 12% of the Earth's surface area.

### 3.5 Mission Timing.

The optimal launch window for CryoSat is 2002-4. This timing is determined by two requirements:

- The extension of the ERS-ENVISAT altimeter time-series of the “interior” regions of the Antarctic and Greenland Ice Sheets depends on having time-coincidence between CryoSat and ENVISAT. The removal of topographic biases through cross-over measurements (§ 2.2) is possible only if the instrument characteristics are unchanged. This will not be the case with ENVISAT and CryoSat. One year of contemporary measurements are required to permit cross-calibration of the CryoSat and ENVISAT altimeters. ENVISAT is launched in 2000. It is nominally a 5-year mission.
- Observations of the US ICESAT are of limited use to estimates of trends at regional scales. On the other hand, the high resolution of the laser sensor will, as cloud cover permits, see detail of sea and land ice roughness at 100 m scales. ICESAT data, where they are available, will be of value in verifying CryoSat performance. One year of contemporary flight with the ICESAT laser altimeter is required to cross-calibrate the altimeters. ICESAT is launched in 2001 with a design life of three years. Although there is an expectation of longer life, there is uncertainty as to the lifetime of the laser diodes. A launch of CryoSat later than 2004 is undesirable.

## 4 Technical Concept

This section describes the CryoSat measurement concept. A qualitative description of the instrument operation is given, followed by a description of the synthetic aperture and interferometric processing of the radar data. This is illustrated with computer simulations. A description of the errors that are expected in the CryoSat observations is given. Illustrations are provided of how these errors are combined in the estimation of areal changes in ice thickness, and these illustrations show why the selected concept may be expected to meet the measurement requirements. The range and likely rate-of-change of important instrument parameters is described. The expected verification activities, and the data processing, are summarised

### 4.1 The Radar Altimeter.

#### 4.1.1 Instrument Concept and Parameters.

The CryoSat altimeter will provide an altimeter system for the ice sheet interiors, for sea ice and for ice sheet margins and other topography. Three operative modes are foreseen:

- Conventional pulse limited operation for the ice sheet interiors (and ocean if desired).
- Synthetic aperture operation for sea ice.
- Dual-channel synthetic aperture/interferometric operation for ice sheet margins.

A qualitative description of how the CryoSat altimeter operates is shown in Box 4.1. Illustrative parameters of the CryoSat altimeter are given in Table 4.1. These parameters provide adequate performance, but other combinations are possible.

**Table 4.1:** Illustrative CryoSat Altimeter Baseline Parameters.

Orbit altitude	650 km
Antenna Full 3 dB beam width	1.2°
Range Resolution	0.46 m
Number of Range Bins	512
Carrier Wavelength	2.2 cm
Interferometer Baseline	1.0
Along-track Synthetic Beam Resolution	300 m
Number of Synthetic Beams	64
Along-track Sampling Interval	300 m
Peak Power	70 W
Antenna Gain	41.5 dB
Noise Figure.	3 dB

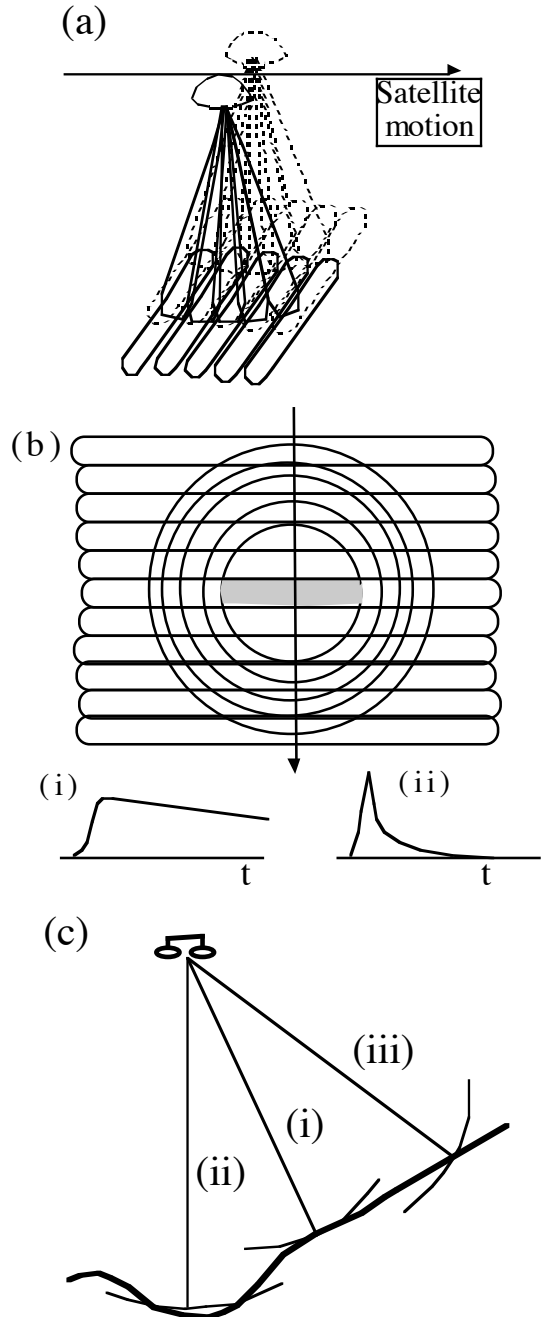


#### Box 4.1 CryoSat altimeter operation.

(a) Synthetic aperture processing is performed on an otherwise conventional Ku-band pulse-limited altimeter to form a set of *e.g.* 64 high-resolution, along-track beams. As the altimeter progresses along its orbit, these beams sequentially scan each sub-satellite area. The altimeter's timing is arranged so that the data from all beams can be combined successively, leading to one height measurement for any given ground location.

(b) *Sea ice operation.* Over a spherical surface, the range rings of the pulse-limited altimeter are divided by the Doppler beams into range slices falling across the track. The area of these falls rapidly with distance across-track. In consequence, the echo no longer takes the familiar pulse-limited form (i), but has a rapid fall (ii). The resolution over a plane surface is the stippled region of the footprint. In our design this is 300 m by 1 km. By determining the location of the leading edge of the echo, the elevation of the central resolution cell is determined. This is the operative mode over sea ice, where differences in the elevation of ice and ocean cells measure the ice freeboard. The 64 echoes at each ground location, (one for each Doppler beam), are multi-looked for speckle suppression.

(c) *Ice sheet operation.* Over ice sheets the surface is not plane, and a method for determining the echo location is required. A second synthetic aperture system is added, as in (a), and used to form an interferometer across the satellite track. The angle of the echo at each range may be determined, and this, together with the range, determines the elevation and across-track location of the surface. The 64 echoes are phase multi-looked to reduce speckle, and to estimate the coherence at each range. When the across-track echo direction is unambiguous, as in (i) or (iii), its coherence is high. Echoes at ranges with ambiguous directions, because two or more points on the surface have the same across-track range, as in (ii), have low coherence, and may be masked. This is described further in the simulations (§3.1.2)



#### 4.1.2 Elevation Retrieval.

Analytic calculations have been carried out (Raney 1995, Raney 1998, Jensen & Raney 1996, Jensen & Raney 1988, Phalippou 1998, Zelli 1998, Phalippou *et al.* 1988, Picardi *et al.* 1988) of echo shapes, along-track beam processing, across-track phase coherence, phase and power multi-looking, and echo phasing and eclipsing. Closed-form calculations are possible only with relatively simple surface geometries, which may not provide an accurate guide to the performance over the more complex sea ice and land ice surfaces. Therefore we do not detail these calculations here, but proceed directly to numerical simulation over the primary mission goal surfaces. Box 4.2 deals with land ice elevation retrieval; Box 4.3 sea ice retrieval.

Details of these numerical calculations are given in Wingham (1997, see also Montefredini *et al.* 1995). These simulations do not include the RF sections of the instrument or the echo timing control. No smoothing has been applied to the elevations, so the data is shown more-or-less as it would appear prior to any higher level processing.

In these simulations, emphasis is placed on the elevation of the first return. This requires explanation. In general, one may treat the across-track surface as a function  $h \equiv h(\theta)$  of across-track angle, so that  $h$  is regarded as the range of the surface at each across-track angle  $\theta$ . The altimeter makes an estimate of the inverse  $\theta(h)$  of this function, in that it samples regularly in range (like a SAR).  $\theta(h)$  is not generally invertible (Box 4.1(c)) and the echo coherence is used to identify the invertible parts of  $\theta(h)$ .  $\theta(h)$  is numerically inverted in the retrieval, (producing the variable coverage in angle observed in Box 4.1.2.1). The error is generally of the form

$$\delta h \equiv -h(\theta) \sin \theta \delta \theta \quad (4.1.1)$$

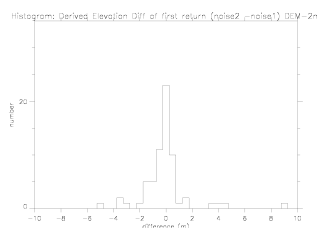
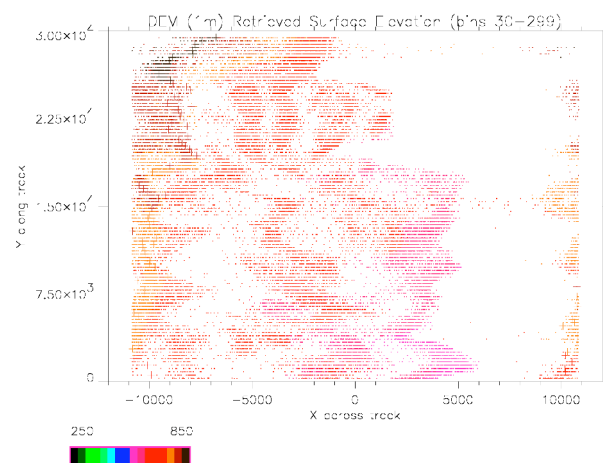
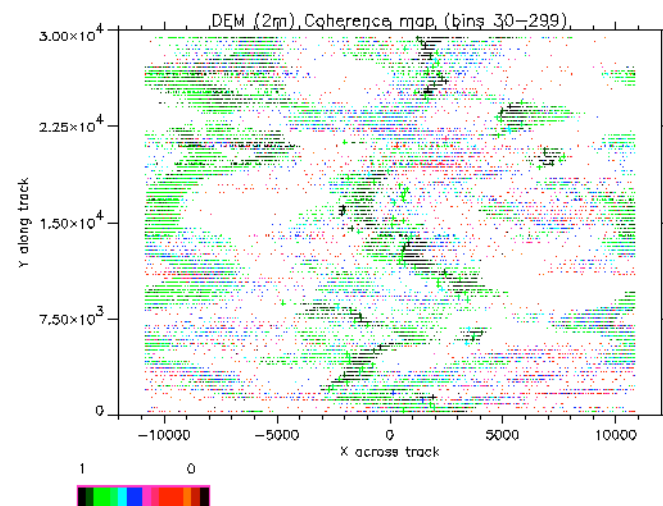
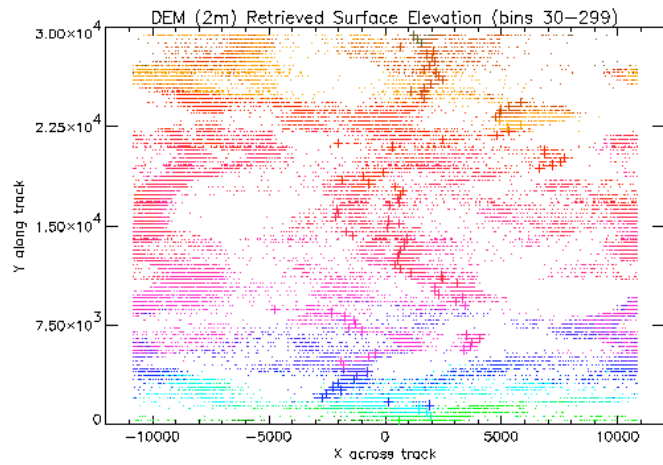
where  $\delta \theta$  is the error in across-track angle. This is the sum of the error in pointing knowledge of the interferometer baseline, and the error in angle measured by the interferometer. The estimates  $h \sim 10^6$  and  $\sin \theta \sim \theta \sim 10^{-2}$  provide  $\delta \theta \sim 10^{-5}$  for a 10 cm error at the edge of the swath. This is the familiar arc-second pointing knowledge requirement of high resolution altimetry. Because the range timing is very accurate, range error is small in comparison and ignored in eqn. (4.1.1).

However, for the earliest echo arrival, the surface is normal to the arrival direction (see Box 4.1 c(i)). In this case,  $h(\theta + \delta \theta) \sim h(\theta) + h(\theta) \sin \theta \delta \theta$  in the vicinity of the point-of closest-approach. At this point, the first order error of eqn. (4.1.1) is cancelled. The elevation error is second-order in  $\delta \theta$  for the first arrival. On the other hand, an error  $\delta r$  arises in determining ("retracking") the first return. To 2<sup>nd</sup>-order in  $\delta \theta$ , the error is

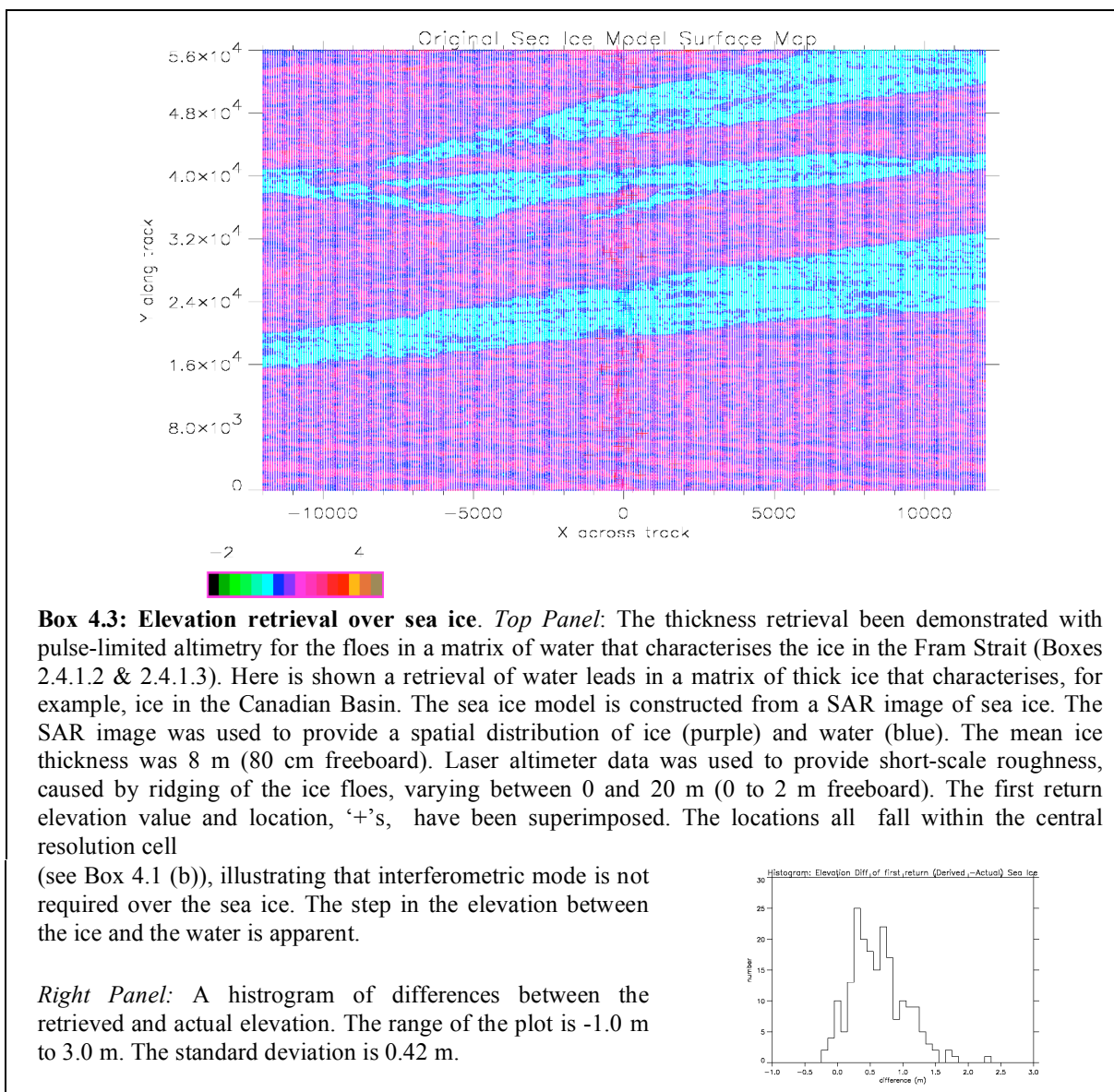
$$\delta h \equiv -h(\theta) \frac{\delta \theta^2}{2} - \delta r \quad (4.1.2)$$

#### Box 4.2: Elevation retrieval over land ice.

*Top:* The retrieved elevation over the Greenland DEM (Box 2.4.3.2) when the altimeter moves up the surface gradient. The crosses show the first return location and elevation. This wanders from side-to-side along the track as the detailed surface geometry changes. Note that it is *not* the function of the altimeter to provide a spatially continuous mapping capability such as SAR interferometry. *2nd panel:* The echo coherence for each of the elevation locations shown above. The black and green regions show high coherence. These correspond to various regions of the surface whose arrival direction is unambiguous. (see Box 3.1.1.1(c)). *3rd Panel:* The retrieved elevation over the Greenland DEM when the altimeter moves across the surface slope. Note that the topography is rotated counter clockwise by  $90^\circ$  with respect to the top panel. The higher topography now falls substantially to the left of the track. Because the across track gradient is large, a small wrapping of the interferometer phase is apparent in the retrieval having placed some locations right of the track. *4th Panel (below):* Histogram of repeat-track differences of first arrival elevations whose coherence exceeds 0.8. The plot scale is -10 to 10 m. The standard deviation is 1.83 m.



For a 10 cm error at the edge of the swath, the pointing error must now be  $10^{-4}$ , or 20 arc-second, which is easier to achieve. On the other hand,  $\delta r$  varies in a complicated way depending on the shape of the surface and the estimation ("retracking") technique. This can only be determined over the surfaces of interest by simulation, which is described in Boxes 4.2 and 4.3.



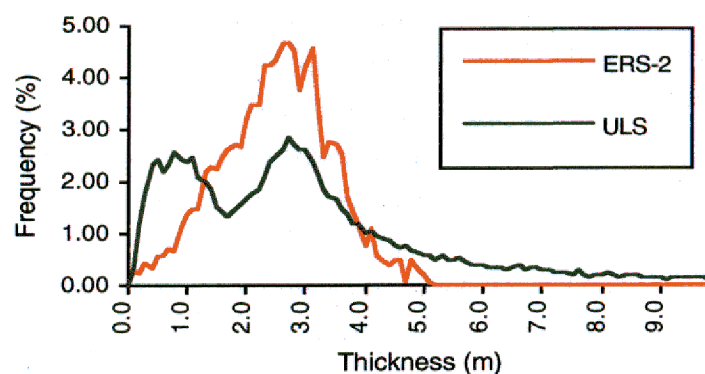
With CryoSat, there is also the question of the affect of penetration on the interferometry. A primary mission goal is to measure sea ice thickness at the end of the summer melt season. Here, penetration of the radar pulse will not be a significant affect in any liquid water is present. Over land ice, however, the pulse will penetrate  $\sim 10$  m into the dry firn of the accumulation zone (Ridley & Partington 1988). However, a simple argument may be given

to show the effect is small. The total volume-scattered power in a Ku-band, normal-incidence echo from dry firn accounts for  $\sim$  half the power, distributed over 10 m or so. Therefore it is around -13dB in any one 0.46 m range bin. This uncorrelated power will degrade the coherence of the range sample. However, the SNR of the simulation in the third panel of Box 4.1.2.1 is around 13 dB, because the energy is from mainly outside the antenna beam, and satisfactory precision is obtained. Penetration will not affect achieving the science requirement.

### 4.1.3 Altimeter Precision and Surface Roughness.

The illustrations of elevation retrieval illustrated in the previous section were performed using a simple threshold algorithm to extract an elevation from the echo power. However, over a surface of known shape and scattering properties, such as the ocean, the precision of an altimeter depends on how closely the noise allows a model of the echo to be fitted to the observations. An elevation precision higher than the range resolution may be obtained in this way. In addition, simultaneous estimates are made of the echo power and the surface roughness. These two latter estimates are used to provide respectively backscattering coefficient, from which the wind-speed is derived, and ocean waveheight. The ERS, ENVISAT, and TOPEX/Poseidon altimeters exploit this principle when operating over the ocean.

**Box 4.4: Sea ice surface roughness from pulse-limited altimetry.**



The ULS data shows that generally, sea ice has a bi-modal thickness distribution. The peak at around 0.8 m is the result of first-year ice, the peak at 3.0 m the result of perennial ice. The perennial ice thickness distribution also has a long tail, stretching to 10 m and above. This long tail is the resulting of ridging, caused by the failure in compression of ice floes. The thickness distribution determined from pulse-limited altimetry is insensitive to the first-year ice, and to the extreme caused by the ridging. CryoSat, with its improved resolution, should provide a better estimate of the perennial ice thickness distribution.

Over the sea ice, the ice thickness distribution is important (Wadhams 1995). Its cause is ridging due to compression of the ice floes. Ridges contain a significant percentage of the mass, control the momentum exchange with the atmosphere, and affect the sea ice rheology (Grey & Morland 1994). With pulse-limited altimetry ice thickness distributions have been



estimated from histograms of the retrieved thickness (Box 4.4). The thickest ridges and thinnest floes are not detected, leading to a bias in the mean thickness. This occurs because the retrieved thickness is an average over the footprint area, and extremes of the ice thickness occur as roughness within the pulse-limited echo. Ice thickness distributions from the CryoSat altimeter should provide an improved retrieval of the thickness distribution. On the other hand, special processing of the CryoSat echoes that takes account of sub-footprint roughness has yet to be investigated in detail.

Over land ice, roughness is a less important parameter for geophysical studies. In addition, ice sheets contain topography at all spatial scales and even the theoretical definition of surface roughness is problematic (Wingham 1995b). Nonetheless, heuristic pulse-fitting procedures (termed ‘retracking’, Martin *et al.* 1983), that account empirically for the broadening of the leading edge from surface ‘roughness’, improve the elevation precision. In its high-resolution mode the CryoSat echo is different from that of a pulse-limited altimeter (Box 4.1(b)). In addition, over topographic surfaces, the echo will depend on the direction of motion of the satellite with respect to the surface because the footprint is not circularly symmetric. Some development of conventional ice sheet procedures is required.

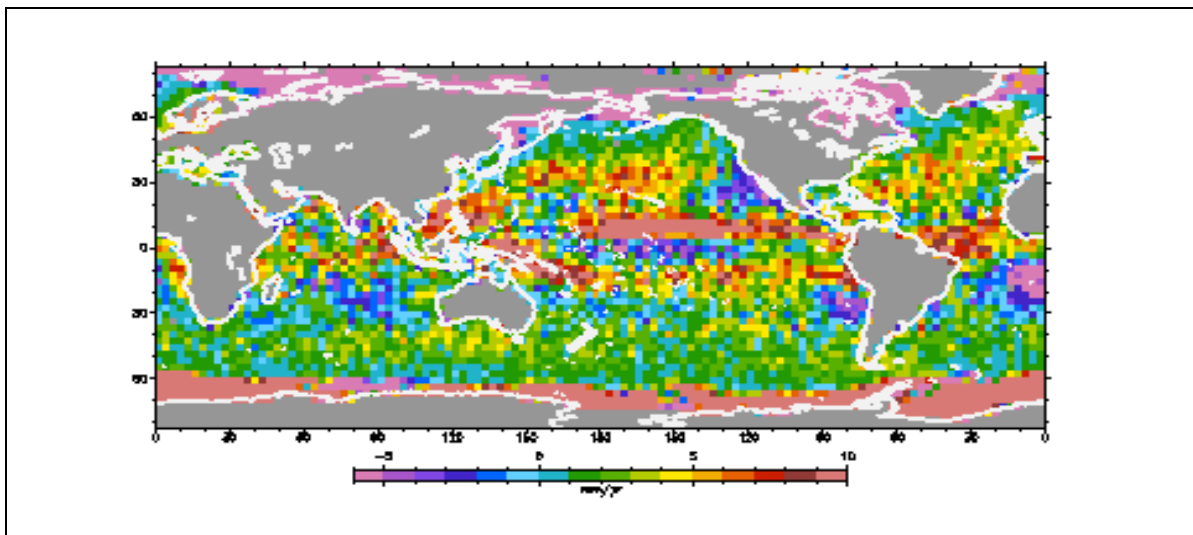
## 4.2. Measurement Error Budget

### 4.2.1 Sea Surface Topography Uncertainty

Because the sea surface is smoothed on scales of 50 km, errors from the atmospheric corrections or the orbit are largely cancelled in eqn. (3.2.7). However, unknown geoid and ocean topography on scales less than 50 km introduce errors in the freeboard measurement. Such topography is clearly seen in the example illustrated in Box. 2.3. CryoSat will allow the formation of a mean sea surface from its (largely) non-repeating tracks. The error at ~ 50 km from sea surface topography will be the difference between this mean surface and the actual sea surface at less than 50 km scales. A comparison with ground-based gravity of the Arctic mean sea-surface generated from the non-repeating ERS Geodetic Mission showed a slope error of  $6 \times 10^{-6}$  radians RMS, almost entirely at scales less than 35 km (Laxon & McAdoo 1998). The equivalent along-track mean sea-surface error is ~ 14 cm at 35 km. The mean dynamic topography in the Arctic is small, of order ~ 2 cm, so this error is largely that due to the measured mean sea surface. The variability of the dynamic topography Arctic Ocean is generally small, of the order 2 cm and dominated by large length scales. The error from this source will generally be small. In the Fram Strait, however, the short-scale topography associated with the East Greenland Current can be significant and an error of ~ 4 cm RMS may be introduced at monthly and 50 km scales (Peacock 1998). Tidal errors have large spatial scales and will be small.

#### 4.2.2 Atmospheric Refraction Uncertainty

In general, the velocity of electromagnetic propagation is affected by the ionosphere, dry atmospheric mass, and atmospheric humidity (see *e.g.* Cudlip *et al.* 1994 and references therein). The largest affect is that due to dry atmospheric mass. This can be removed from the range measurement to order millimetres by modeling. We assume any residual error is small. The ionospheric correction is variable but small in polar regions. We assume errors arising in long trends are small. (Over Antarctica, the total correction is barely worth making.) The largest error is likely to be that due to the atmospheric humidity, which can vary significantly in time and space. Most altimeter satellites carry a microwave radiometer to provide a measurement of water vapour. However, over ice surfaces this instrument does not provide accurate results. Thus CryoSat will not carry a radiometer and an atmospheric delay error will result. From Box 4.5 shows, this error is likely to be of order  $1.0 \text{ cm yr}^{-1}$  at  $10^4 \text{ km}^2$  and  $0.5 \text{ mm yr}^{-1}$  at  $10^7 \text{ km}^2$ .



**Box 4.5: Wet troposphere errors.** We compared modelled (ECMWF) and measured (MWR) wet tropospheric path delays for 3 years of ERS-2 data (1995-1998). We computed differences between modelled and measured values, averaged these in 35-day batches over  $3 \times 3$  degree cells ( $\sim 10^5 \text{ km}^2$ ), and passed trends through the averages. These trends are largely due to the modelled field errors. The extremes of the colour bar are  $-0.5$  and  $1.0 \text{ cm yr}^{-1}$ . At high latitudes (except in regions of sea ice contamination of the MWR) the trends are very small,  $\sim 0.1 \text{ cm yr}^{-1}$ . A worst case assumption is that trends at scales larger than  $10^4 \text{ km}^2$  are independent, in which case the trends will be order  $\sim 0.3 \text{ cm yr}^{-1}$  at  $10^4 \text{ km}^2$ . At  $10^7 \text{ km}^2$ , we comfortably expect this error to be less than  $0.05 \text{ cm yr}^{-1}$ . At latitudes higher than those shown, the correction becomes very small due to the low atmospheric temperatures.

#### 4.2.3 Orbit Error.

CryoSat will rely on the Global Positioning System (GPS). The GPS receivers allow precision orbit determination with an 6 cm RMS accuracy in the radial component at wavelengths of 40000 km and less. The main contribution to this error is gravity model errors and it may come down to 2 cm due to improving gravity models the time of the mission. Taking advantage of the large number of GPS tracking data that will be available,

reduced-dynamic orbit determination techniques can be employed, which makes the orbit determination virtually a geometric problem. Recent experiences with TOPEX/POSEIDON have demonstrated that radial orbit precision of 2 cm are readily available using GPS tracking (Bertiger *et al.* 1994, Melbourne *et al.* 1994). Although TOPEX/POSEIDON flies in a higher orbit, similar orbit precisions may be achieved for CryoSat when the tracking abundances allow the reduction of the dynamic model errors. Long-term orbit stability can be achieved with GPS. Any GPS-induced instabilities in the orbit can be monitored by other satellites flying GPS receivers in conjunction with other tracking data types, like TOPEX/POSEIDON and Jason-1. Even with ERS-1, using laser ranging, stability over the Southern Ocean over a three years was of order 0.1 cm yr<sup>-1</sup> in comparison with TOPEX (Wingham *et al.* 1998).

#### 4.2.4 Orbit Pattern and Vertical Accuracy

The measurement requirements of CryoSat specify the error arising from spatial averages of individual CryoSat observations. To illustrate how the orbit and instrument accuracy requirements may be determined, we assume an orbit inclination of 86°. This orbit satisfies the spatial extent requirement (§ 3.4.5) and the allowable data loss at the poles (§ 3.4.1). We assume a repeat period of 1 year, with a sub-cycle of 1 month. The track spacing is ~ 70 km at 50° latitude, and ~ 5 km after 1 year. The orbit satisfies the spatial and temporal sampling requirements of § 3.4.4. We assume a mission duration of three years.

Over sea ice the measurement accuracy is that obtained from passing a trend through  $N$  late summer average observations over the mission lifetime. We shall term the error associated with one of these observations the vertical accuracy, denoted  $\bar{\sigma}_v$ . The relation between the vertical accuracy and the measurement accuracy is of the form

$$\bar{\sigma}_m = \bar{\sigma}_v \sqrt{\frac{12}{N(N-1)(N+1)}} \times \left( \frac{1}{1 \text{ year}} \right) \quad (4.2.1)$$

and if the mission duration is 3 years,  $N$  equals in this formula. The vertical accuracy of a summer or annual average is then in either case  $\sqrt{2}\bar{\sigma}_m \times 1 \text{ year}$ . For sea ice the measurement requirement is 1.6 cm yr<sup>-1</sup> at 10<sup>5</sup> km<sup>2</sup>, which gives a vertical accuracy of 2.3 cm at 10<sup>5</sup> km<sup>2</sup>.

Over sea ice, measurements will be made from differences in along-track observations of the ocean and ice surfaces. The vertical accuracy will take the form

$$\bar{\sigma}_v^2 = \frac{\sigma_i^2}{(1-f_i)f_i(1-f_i)N_t} + \bar{\sigma}_{oc}^2 + \bar{\sigma}_b^2 \quad (4.2.2)$$

where  $N_t$  is the total number of observations,  $f_i$  is the fractional ice concentration (proportion of the ocean surface covered by ice),  $f_l$  the fractional loss resulting from



unclassifiable pulses, and  $\sigma_i$  is the instrument single-shot precision.  $\sigma_{oc}$  is the net result at  $10^5 \text{ km}^2$  of the 50 km scale geoid and dynamic topography uncertainty (§ 4.2.1).  $\bar{\sigma}_b$  is a bias that we assume present due to the differing echo shapes of ice and water. It is removed through external calibration (§ 4.4).

For the illustrative orbit we have assumed in this section, the number of ascending and descending tracks in  $10^5 \text{ km}^2$  in one month at  $50^\circ$  latitude is  $\sim 9$ , with a total length of  $\sim 3000 \text{ km}$ . We assume an ice concentration of 70% and a data loss of 20% due to small floes or leads. Using the results of § 4.2.1,  $\bar{\sigma}_{oc}$  is 1.59 cm at  $10^5$ . Taking the along-track sampling interval to be 0.3 km, the number of observations is 10000 in this illustration. With these values, eqn. (4.2.2) requires the radar precision to satisfy

$$\sigma_i < 0.66 \text{ m} \quad (4.2.4)$$

to meet the vertical accuracy requirement. In comparison, the histogram of the difference between the retrieved elevation and the actual surface elevation provided by the simulation of Box 4.1.2.2 is 0.42 m, which meets the requirement of eqn. (4.2.4).

Turning now to the case of land ice, the refraction error (§ 4.2.2) is present and allowance must be made for it. At  $10^4 \text{ km}^2$ , the measurement requirement is  $3.6 \text{ cm yr}^{-1}$ . The refraction error is estimated to be  $1 \text{ cm yr}^{-1}$ , so the requirement in the absence of refraction is  $3.5 \text{ cm yr}^{-1}$ . At a scale of  $13.8 \times 10^6 \text{ km}^2$  the measurement requirement has a value of  $0.5 \text{ cm yr}^{-1}$  and the refraction error estimated to be  $0.05 \text{ cm yr}^{-1}$ , which is negligible, so the requirement in the absence of refraction is  $0.5 \text{ cm yr}^{-1}$ . Over land ice the measurement accuracy is again that obtained from passing a trend through  $N$  average observations over the mission lifetime, and again, with this example orbit,  $N = 3$ . The vertical accuracy  $\bar{\sigma}_v$  of the annual averages is then 4.9 cm and 0.7 cm.

Over land ice, elevation differences at cross-over locations are used. The vertical accuracy has the form

$$\bar{\sigma}_v^2 = \frac{\sigma_i^2}{N_x} + \bar{\sigma}_o^2 + \bar{\sigma}_b^2 \quad (4.2.5)$$

where  $N_x$  is the number of cross-overs,  $\bar{\sigma}_o$  is the orbit accuracy and  $\bar{\sigma}_b$  is a bias that we assume present due to changing surface-to-volume scattering ratio in dry firn (Wingham *et al.* 1988, Legresy & Remy 1998). It is removed by correlation of observed elevation and power changes (§ 4.5). Because cross-overs are used, the variable part of the orbit error is substantially decorrelated, and the orbit error takes the form

$$\bar{\sigma}_o^2 \sim \frac{\sigma_o^2}{N_x} + \bar{\sigma}_{ob}^2 \quad (4.2.6)$$

where  $\bar{\sigma}_{ob}$  is the unknown orbit drift. At  $10^4 \text{ km}^2$  it is negligible. In this orbit, the number of cross-over pairs in  $10^4 \text{ km}^2$  in one year at  $63^\circ$  (the southern limit of Greenland) is  $\sim 1000$ . The radar and orbit precision must satisfy

$$(\sigma_i^2 + \sigma_o^2)^{1/2} < 155 \text{ cm} \quad (4.2.7)$$

to satisfy the measurement requirement. With a conservative estimate (§ 4.2.3) for the orbit error  $\bar{\sigma}_o$  of 6 cm, one has for the requirement on instrument precision a value of 154 cm.

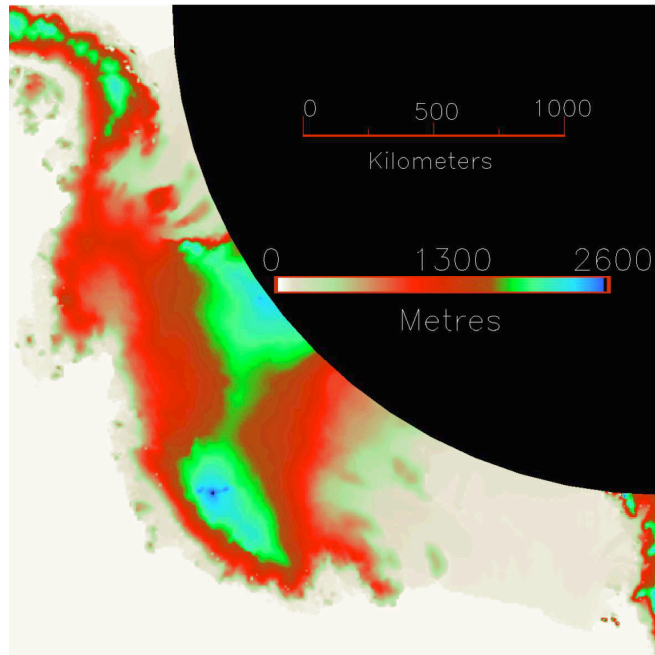
In comparison, the histogram of the along-track repeatability of the retrieved elevation provided by the simulation of Box 4.1.2.2 is shown in the box. The standard deviation of the first-arrival differences is 1.83 m, implying a precision  $\sigma_i$  of 1.29 m.

At  $13.8 \times 10^6 \text{ km}^2$ , the number of cross-overs will be at least 1000 time larger. If eqn. (4.2.7) is satisfied at  $10^4 \text{ km}^2$  the instrument and orbit precision will contribute 0.15 cm to the vertical accuracy. The orbit drift  $\bar{\sigma}_{ob}$  is of greater importance at these scales, but (§ 4.2.3) is likely to be of order  $0.1 \text{ cm yr}^{-1}$  over 3 years. The measurement requirement is 0.7 cm. This calculation illustrates that it is the measurement requirement at short spatial scales that is most challenging.

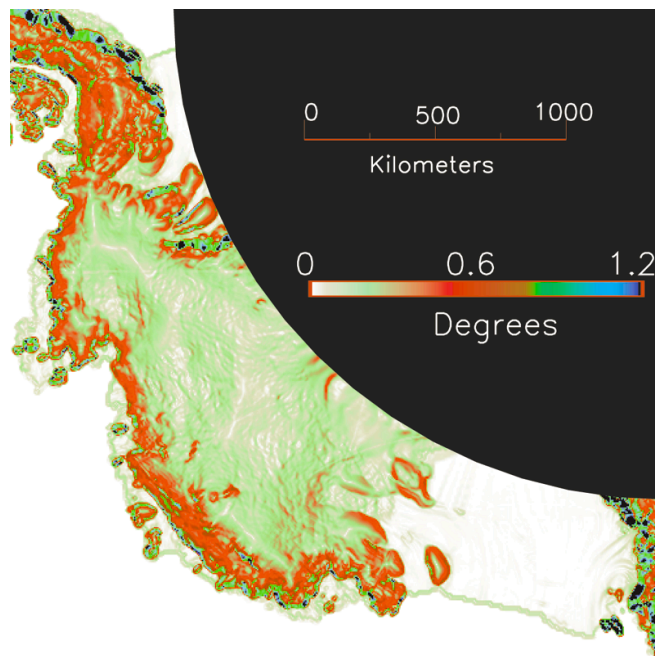
### 4.3 Echo windowing requirements.

The retrieval illustrated in Box 4.1 depends on having available the first arrival of the radar echo and a sufficient echo duration to accommodate the slant range of the Doppler beams. On the other hand, the range of first-arrival times that occurs around the orbit, due to the orbit and to the surface topography, greatly exceeds that needed to accommodate the slant range of the Doppler beams. For this reason, the echo is windowed to reduce the instrument data rate. With full-deramp processing, the positioning of the window in echo delay-time depends upon knowing the echo delay prior to its arrival. This is accomplished with a “tracker”, which estimates the delay of the echo first arrival.



For the purposes of tracker design, it is necessary to place requirements on: (a) the range of delay times over which the position of the window may vary, (b) the rate at which the position of the window may vary, and (c) the range of first arrival times that may be expected to fall within the window at any given location around the orbit. The first two these, (a) and (b), are largely determined by the large-scale surface topography (and variations arising from the orbit), and the third, (c), is largely determined by the surface slopes on the scale of the antenna footprint.



**Box 4.6: The elevation of West Antarctica.** At the scale and hydrostatic pressures of ice sheets, ice behaves as a plastic fluid. In consequence the topography is characterised by large inland areas with very little topography, bounded by marginal regions of rapidly varying elevation. In some areas, such as the Antarctic Peninsular (top left), the topography is complicated by mountains protruding through the ice, leading to a greater range of topography within the ice sheet interior.



**Box 4.7: The gradient of West Antarctica.** The interior of the ice sheet, with the exception of the mountainous Antarctic Peninsular, exhibits slopes of less than  $0.6^\circ$ . In the marginal regions, the slopes increase rapidly. This figure was derived from ERS altimeter data, which fails to observe slopes larger than  $1.2^\circ$ . Values of slope greater than  $1.2^\circ$  are suppressed in the figure. At the margins, and around the Antarctic Peninsular, the terrain is mountainous, and slopes in excess of  $5^\circ$  occur widely.

		Issue: 1 Date: 21. September 1999 Page: 39
---	---	--

For CryoSat, the secondary objectives demand that all of the Earth's topography lying above and at sea-level may be observed, and a range of topography of  $-100$  m to  $+9000$  m with respect to the ellipsoid should be foreseen. The rate at which this topography may vary around the orbit may be estimated for the Antarctic continent, a primary mission goal surface, from Box 4.6. The spatial distribution of surface slopes in Antarctica is described in Box 4.7. It should be noted that, while the area of surfaces with slopes exceeding  $1^\circ$  is small, these are of particular significance to mass imbalance studies and ice dynamic studies (Box 2.5). The tracker design should seek in particular to accommodate these surfaces.

#### **4.4 Radiometric and Fidelity Requirements.**

##### **4.4.1 Range of Backscattering Coefficient and Dynamic Range.**

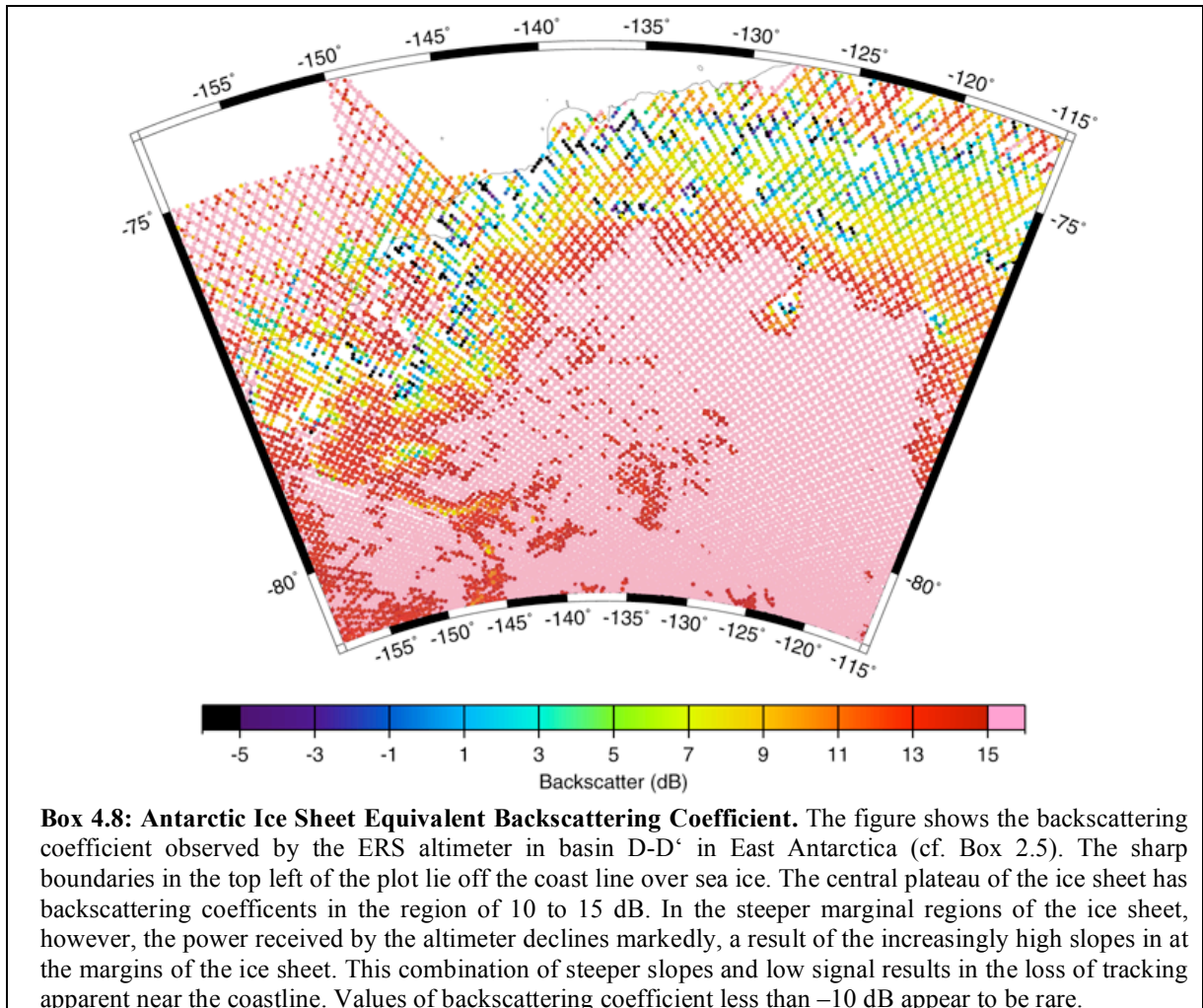
At normal incidence and  $\sim 14$  GHz, ice has a backscattering coefficient of around 11 dB, although this may vary by several dB as a result of surface geometry at the scale of a wavelength. However, in the steeper margins of ice sheets, the area of the surface contributing to a range cell may decline considerably, with the result that the echo power also declines. For the purposes of signal-to-noise calculations, therefore, it is more useful to use the effective backscattering coefficient, defined to be the backscattering coefficient of a plane surface that would result in the received power observed in the range gate. At the margins of ice sheets (Box 4.8), values lying between 0 and 10 dB are common. Values less than  $-10$  dB appear rare.

At the opposite extreme, very high values of backscattering coefficient may be observed from sea ice in calm conditions. The presence of ice prevents the propagation of waves on the ocean surface, which can in consequence take on a mirror-like behaviour. Values of backscattering coefficient of 40 dB are common. Values exceeding 55 dB are rare.

Over smooth regions of the ice sheet the power in land ice echoes does not generally vary rapidly as a function of position (Box 4.8). Over the marginal regions, the power fluctuations can increase, because the power depends largely on the instantaneously illuminated area which can be a rapidly varying function of range and position. Variations of 20 dB may be anticipated, although larger variations may occur. The echo power from sea ice can vary considerably on scales of a few km (Box 2.3), in extreme cases by over 40 dB in a few km.

These power variations need to be taken into account in forming the instrument design, and in particular the receiver instantaneous dynamic range, the range ambiguities and the azimuth ambiguities. While the altimeter may be equipped with a gain control loop to accommodate power fluctuations, the instantaneous dynamic range must accommodate fluctuations which occur over along-track distances which are shorter than the distance travelled in the control loop response time. Range ambiguities will be important for rapid variations of echo power in delay. These are of most concern over complex land ice topography. Azimuth ambiguities are important for rapid variations in position. This is of particular concern over

sea ice. The distinction of ice and water depends on their difference in backscattering coefficient (Box 2.3)



A dynamic range and range and azimuth sidelobe suppression of 40 dB should cover all cases<sup>7</sup>. It is recognised, however, that there may be practical difficulties in meeting this requirement, and some further investigation is required to determine whether a smaller range or suppression is sufficient.

#### 4.4.2 Echo Fidelity.

In conventional ocean altimetry, the echo shape is more-or-less known. In consequence, signal distortions (such as unwanted harmonics from mixers, for example) can be

<sup>7</sup> It should be noted that the fluctuations in power in the time-domain at the A/D convertor of a full-deramp altimeter are smaller than those that occur in the frequency domain, because the very bright echoes observed over sea ice occupy only a few range gates. Advantage of this may be taken in specifying the A/D convertors.



accommodated to some extent by after-the-fact calibration. The CryoSat altimeter, however, will have to accommodate a great range of echo shapes and signal levels, and linearity of the echo recording is important. To consider this further, write the echo as  $f(x, t)$ , and the recorded echo as  $a(x)\hat{f}(x, t)$ , where  $a(x)$  is the gain and  $\hat{f}(x, t)$  the signal that appears in the range window. Suppose that  $f(x, t)$  includes the linear distortions of the range impulse response. If the system were perfectly linear, then one would have  $a(x)\hat{f}(x, t) = f(x, t)$ . In general, however, the system is imperfect, and we suppose that the actual recording is of the form  $(a(x) + \delta a(x))(\hat{f}(x, t) + \delta \hat{f}(x, t))$ . The distortions that result are then

$$\begin{aligned} & (a(x) + \delta a(x))(\hat{f}(x, t) + \delta \hat{f}(x, t)) - a(x)\hat{f}(x, t) \\ & \sim \delta a(x)\hat{f}(x, t) + a(x)\delta \hat{f}(x, t) \end{aligned} \quad (4.4.1)$$

We term the first of these terms multiplicative errors, the second additive errors.

With regard to multiplicative errors, there is no mission requirement for absolute values of backscattering coefficient. On the other hand, the stability of the measurement of received power is important. Changes in received power over the mission lifetime are important in determining biases in the land ice elevation change resulting from volume scattering (§ 4.4). The sensitivity of the elevation change to power change is of the order of 0.4 m/dB (Arthern 1996). The measurement requirement over the ice sheets is  $0.5 \text{ cm yr}^{-1}$ . Biases from unknown variations in received power should be small in comparison; at worst they should not exceed 0.05 dB over a 3 year mission.

In general the measurements are fairly tolerant of stable multiplicative errors which are a slow function of the gain  $a(x)$ . There are two considerations. The distinction between sea ice and ocean depends on discriminating their backscatter coefficients. A precise requirement in this respect is hard to give, but errors larger than 1 dB should be avoided. Secondly, empirical correlation between echo power change and elevation change is used to correct the data, and these would become difficult if  $\delta a(x)$  exceeded 0.1 dB within a 10 dB range of  $a(x)$ .

The measurements are less tolerant of additive errors. Distortions in echo shape can confuse the elevation estimation. In general these should be small in comparison with the linear distortions of the range impulse response (with the exception of the ends of the range window where some aliased energy may occur).

#### 4.5 Verification Activities.

The scientific utilisation of the data will aim to provide digital maps of the variations in time and space of the fluxes of sea ice thickness and mass and land ice thickness and mass change. Examples of these are shown in Boxes 2.2 and 2.5. These products make use of repeat-track and cross-over analyses. Their starting point is (at least) 1 month of data. We anticipate from experience that over large temporal or spatial scales, biases will emerge in

these higher level products from a variety of sources. These biases are dealt with by external verification, and we consider these here.

Over sea ice, differences in echo shapes from the ice and water will generally lead to a freeboard bias. In the case of pulse-limited altimetry, the comparison (Box 2.4) of the altimeter and ULS thickness shows a bias of 0.2 m thickness (2 cm freeboard), assuming the ULS is perfect. The poor resolution of the pulse-limited altimeter precludes a detailed understanding of this bias, and CryoSat will have a smaller bias. Nonetheless a residual bias may be foreseen. Therefore the ULS data (the only permanent ground data) will be important to determining the bias. There are also questions which require detailed ground campaigns, coincident with CryoSat observations. Sea ice roughness is an important parameter, in that a significant proportion of mass is contained in ridges, and these control the momentum transfer from the atmosphere to the ice. We are currently working on the estimation, in the statistical sense, of sea ice roughness (Box 4.4), and ground validation of these algorithms is important.

We intend (at least) one summer campaign in the Arctic aimed at providing ground and airborne measurements coincident with CryoSat observations. These observations will include the use of the airborne Applied Physics Laboratory Delay/Doppler radar, (essentially similar to the CryoSat sea ice mode), together with the University of Helsinki airborne laser altimeter and NERSC ship-borne equipment for sea ice measurements. Coincident SAR data from ENVISAT will also be employed, and, should cloud-free data be available, ICESAT observations.

Over land ice, verification activities are planned at the Greenland Grip Core site, where an extensive array of GPS receivers are maintained by KMS, Denmark, and detailed topographic information is available from previous surveys (Forsberg *et al.* 1992). Airborne SAR and laser altimeter data will also be available at this site. In Antarctica, verification of the CryoSat elevations will be performed using the Alfred Wegener Institute GPS observations on the Ronne-Filchner Ice Shelf, together with tidal measurements from British Antarctic Survey. A combination of these measurements was used to verify ERS-1 ice sheet elevations as part of the CEC ESAMCA project (Wingham 1994). Over land ice, we also anticipate a time-variant bias in cross-over measurements (Arthern 1996, Legresy & Remy 1998) due to variations in surface-to-volume scattering ratio. This is removed by cross correlation with the time variation in signal power, to which it is linearly related (Wingham *et al.* 1998). We anticipate a similar correction with CryoSat.

The commissioning phase of the CryoSat mission should ensure the entire mission system will meet the science requirements, as specified in § 3.1.2. We foresee a commissioning phase of 3 months duration. Ice sheet cross-overs with ENVISAT will be used for cross-calibration of the two systems. It should be noted that the precise timing of the CryoSat launch may require the commissioning phase, a post launch activity, and the verification phase, which is tied to the Northern Hemisphere summer, to be separated in time. It should also be foreseen that during the verification phase, a short repeat orbit (3 days for example) will be required.



#### 4.6 Data Product Requirements

The principal output of the CryoSat are maps of variations in sea and land ice fluxes (e.g. Box 2.5). These will follow from a “Processing” stage and a “Data Utilisation” stage. (These terms have the meanings given in Table 3 of the ESA Opportunity Mission Announcement of Opportunity). These scientific products will utilise a lower level product, a sensor data product (“SDR”), which will be the principal output of the Processing stage.

Raw data will be converted to data products (§ 3.4.1) in two steps: a level 0 product, and two level 1b products, the SDR and GDR. The level 0 data is raw telemetry reformatted into instrument source packets (ISPs) and annotated with an orbit state vector file, a UTC to satellite binary time (SBT) conversion file, and a configuration file. This data will be archived.

##### **Box 4.9: An example illustrating a possible CryoSat SDR data product**

will be a time-ordered, corrected, calibrated, quality controlled, Earth-located waveform product:

1 Hz data block containing:



- UTC time and location in an ellipsoidal reference frame; Ionosphere Correction, Dry Troposphere Correction, Wet Troposphere Correction, Internal Range Calibration, Range and Gain Control Values, Range-rate and Gain-rate Control Values; Instrument Modes; Instrument Range Resolution; Land/Ice/Ocean Flag.

25 Hz data block containing:

- 512 waveform samples; 512 phase angles; 512 coherence values; 512 elevation values; Retracked first-arrival elevation value; Retracked peak power; Retracked Pulse-peakiness; Retracked Roughness.

together with quality control and data blocking information.

Level 1b data processing decodes the instrument telemetry, applies instrument pre- and post-launch characterisation data, atmospheric correction data, and Earth location data, and performs waveform estimation and product formatting. CryoSat demands external data provision for Earth location and atmospheric correction (§ 2.3.3) of the data. As baseline we will use ECMWF pressure and humidity fields for the dry and wet atmospheric corrections (see e.g. Cudlip 1994) and the International Reference Ionosphere (IRI) model (Bilitza et al. 1995) for tropospheric corrections. Earth location will use GPS-derived orbits. The CryoSat-specific waveform processing consists of Doppler beam formation on in-phase and quadrature components from each receiving chain, phase and power multi-looking, and first-return retracking and waveform parameter (range, power and peakiness) estimation. Optimal estimators for the first-arrival time and surface roughness (§ 4.1.3) are the subject of present study. For illustrative purposes only, an example of a possible SDR product is described in Box 4.9.



		Issue: 1 Date: 21. September 1999 Page: 44
---	--	--

The data has no timeliness requirement. It will be distributed to scientists for higher-level processing (*i.e.* repeat-track and cross-over processing). Regional masking of the data should be foreseen. With ERS experience, we anticipate distribution to  $\sim 15$  laboratories. A second product is foreseen for wider distribution (the “GDR”)<sup>8</sup>, comprising, for example, 1 Hz data and 25 Hz retracked values.

---

<sup>8</sup> The terms sensor data record (SDR) and geophysical data record (“GDR”) are borrowed from Seasat altimeter definitions.

---

		Issue: 1 Date: 21. September 1999 Page: 45
---	---	--

## 5. Bibliography

- Aagaard, K., 1994, "The Arctic Ocean and Climate: A Perspective", Geophysical Monograph **85**, 5 - 20, American Geophysical Union.
- Aagaard, K., & E.C. Carmack, "The role of sea ice and other fresh water in the Arctic circulation", J. Geophys. Res., **94**, 14485 - 14498.
- ACSYS, 1998, "ACSYS Initial Implementation Plan", <http://www.npolar.no:80/acsys/projdes.html>.
- Alley, R.B. and I.M. Whillans, 1991, "Changes in the West Antarctic Ice Sheet", Science, **254**, 959 - 963.
- Arthern, R.J., 1996, Ph.D. Thesis, University of London.
- Beltley, C.R., and M. B. Giovinetto, 1991, "Mass balance of Antarctica and Sea Level Change", in Role of the Polar Regions in Global Change, University of Alaska, Fairbanks, pp 481 - 488.
- Bertiger, Y. E. & 19 co-authors, 1994, "GPS precise tracking of TOPEX/Poseidon: Results and implications", J.Geophys.Res., **99**, 24449-24464.
- Bilitza, D., C. Koblinski, B. Beckley, S. Zia & R. Williamson, 1995, "Using IRI for the computation of ionospheric corrections for altimeter data analysis", Advances in Space Research, **15**, 113 - 119.
- Bond, G., W. Broecker, S. Johnsen, J. McManus, L. Labeyrie, J. Jouzel & G. Bonani, 1993, "Correlations between climate records from North Atlantic sediments and Greenland ice", Nature, **365**, 143-147.
- Broecker, W.S., 1994, "Massive iceberg discharge as triggers for global climate change", Nature, **372**, 421 - 424.
- Chao, B.F., 1994, "Man-made lakes and sea level rise", Nature, **370**, 258.
- Colman, R.A., S.B. Power, B.J. MacAveney and R.R. Dahni, 1995, "A non-flux corrected transient CO<sub>2</sub> experiemnt using the BMRC coupled ocean atmosphere GCM", Geophys. Res. Lett., **22**, 3047 - 3050.
- Comiso, J.C., P. Wadhams, W.B. Krabill, R.N. Swift, J.P. Crawford & W.B. Tucker, 1991, "Top/Bottom Remote Sensing of Arctic Sea Ice", J. Geophys. Res., **96**, 2693 - 2709.
- Cubash, U., K. Hasselmann, H. Hock, E. Maier-Reimer, U. Mikolajewicz, B.D. Santer and R. Sausen, 1992, "Time dependent greenhouse warming computations with a coupled ocean-atmosphere model", Clim. Dyn., **10**, 1 - 19.
- Cudlip, W., and 12 co-authors, 1994, "Corrections for altimeter low-level processing at the earth Observation Data Centre", Int. J. Remote Sensing, **15**, 889 - 914.
- Dickson, R.R., J. Meincke, S.-A. Malmberg & A.J. Lee, 1988, The "Great Salinity Anomaly" in the Northern Atlantic 1968 - 1982", Prog. Oceanography, **20**, 103 - 151.
- Eicken, H., M. Lensu, M. Lepparanta, W.B.Tucker III, A.J. Gow and O. Salmela, 1995 "Thickness, structure and properties of level summer multi-year ice in the Eurasian sector of the Arctic Ocean", J. Geophys. Res., **100**, 22697-22710.
- Enomoto, H., 1991, "Fluctuations of snow accumulation in the Antarctic and sea level pressure in the Southern Hemisphere in the last 100 years", Climatic Change, **18**, 67 - 87.
- ESA, 1996, "The Topography Mission: Report for Assessment", ESA SP-1196(9).
- ESA, 1998, The Earth Explorer Program: The Science and Research Element of ESA's Future Earth Observation Program", ESA-SP-1227.

- Farrell, W.E. and J.A. Clarke, 1976, "On post-glacial sea level", *Geophys. J. Roy. Astron. Soc.*, **46**, 647 - 667.
- Fischer, H. & P. Lemke, 1991, "On the required accuracy of atmospheric forcing fields for driving dynamic-thermodynamic sea ice models", in *Geophysical Monograph* **85**, 373 - 381, American Geophysical Union.
- Flato, G.M., & Hibler, W.D., 1992, "Modeling pack ice as a cavitating fluid", *J. Phys. Ocean.*, **22**, 626 - 651.
- Forsberg, R., S. Ekholm, K. Keller & D. Burtin, 1992, "GPS measurements in Greenland in support of gravity measurements and satellite altimetry", *Proc. 6th Int. Symp. on Satellite Positioning*, Columbus, Ohio, pp 905 - 914.
- Gates, W.L., & 9 co-authors, 1996, "Climate Models- Evaluation", in *Climate Change 1995, The Science of Climate Change*, Cambridge University Press.
- Gloersen, P., W. J. Campbell, D. J. Cavalieri, J. C. Comiso, C. L. Parkinson, and H. J. Zwally, 1992, *Arctic and Antarctic Sea Ice, 1978-1987: Satellite Passive-Microwave Observations and Analysis*, NASA SP-511, NASA, Washington DC, 1992.
- Gornitz, V., S. Lebedeff and J. Hansen, 1982, "Global Sea Level Trends in the Past Century", *Science*, **215**, 1611 - 1614.
- Gorshkov, S.G., 1983, *World Ocean Atlas, Vol. 3, Arctic Ocean*, Pergamon, New York.
- Grey, J.M.N. & L. W. Morland, 1994, "A two-dimensional model for the dynamics of sea ice", *Phil. Trans. Proc. Roy. Soc. Lond.*, **347**, 219 - 290.
- Haeberli, W. and M. Hoelzle, 1995, "Application of inventory data for estimating characteristics of and regional climate change effects on mountain glaciers - a pilot study with the European Alps", *Ann. Glaciology*, **21**, 206 - 212.
- Hansen-Bauer, I., 1992, "The Climate of Halley - Antarctica", *DNMI Report*, No. 3/92 Aurora and 26/92 Klima, 22 pp.
- Harder, M., P. Lemke and M. Hilmer, 1998, "Simulation of sea ice transport through Fram Strait : Natural variability and sensitivity to forcing", *J. Geophys. Res.*, **103**, 5595-5606
- Hibler, W.D., 1979, "A dynamic thermodynamic sea ice model", *J. Oceanography*, **9**, 815 - 846.
- Horel, J.D., and J.M. Wallace, 1981, "Planetary scale atmospheric phenomena associated with the interannual variability of sea surface temperatures in the equatorial Pacific", *Mon. Weather Rev.*, **109**, 813-829.
- Hughes, T., 1981, "The weak underbelly of the West Antarctic Ice Sheet", *J. Glaciology*, **27**, 518 - 525.
- Huybrechts, P., 1990, "A 3-D model for the Antarctic Ice Sheet: a sensitivity study on the glacial-interglacial contrast", *Climate Dynamics*, **5**, 79 - 92.
- Huybrechts, P., 1994, "The present evolution of the Greenland Ice Sheet: an assessment by Modeling", *Global Planetary Change*, **9**, 39 - 51.
- Ip, C.F., W.D. Hibler & G.M. Flato, 1991, "On the effect of rheology on seasonal sea ice simulations", *Ann. Glaciology*, **15**, 17 - 25.
- Jacobs, S.S, H.H. Helmer, C.S.M. Doake, A. Jenkins & R.M. Frolich, 1992, "Melting of ice shelves and the mass balance of Antarctica", *J. Glaciology*, **38**, 375 - 387.
- Jensen, J. R. and R. K. Raney (1998), *Delay/Doppler Radar Altimeter: Better Measurement Precision*, *Proceedings IEEE International Geoscience and Remote Sensing Symposium IGARSS'98*, Seattle, Washington, USA, IEEE No. 98CH36174, July 1998, pp. 2011-2013.



- Jensen, J. R. and R. K. Raney (1996), Multi-Mission Radar Altimeter: Concept and Performance, Proceedings IEEE International Geoscience and Remote Sensing Symposium IGARSS'96, Lincoln, Nebraska, USA, IEEE No. 98CH36174, May 1996, pp. 2011-2013.
- Johannessen, O.M., M. Miles & E. Bjorno, "The Arctic's shrinking sea ice", *Nature*, **367**, 126 - 127, 1995
- Laxon, S.W., & D. McAdoo, 1994, "Arctic Ocean gravity field derived from ERS-1 satellite altimetry", *Science*, **256**, 621 - 624, 1994.
- Laxon, S.W. & D. McAdoo, 1998, "Satellites provide new insights into polar geophysics", *EOS Trans.*, **79**, 69 - 73.
- Legresy, B. & F. Remy, 1998, "Using the temporal variability of satellite radar altimetric observations to map surface properties of the Antarctic Ice Sheet", *J. Glaciology*, in press.
- Le Meur, D.E. & P. Huybrechts, 1998, "Present-day uplift patterns over Greenland from a coupled ice sheet / visco-elastic bedrock model", *Geophys. Res. Lett.*, **25**, 3951 - 3954.
- MacAyeal, D.R., 1992, "Irregular oscillations of the West Antarctic Ice Sheet", *Nature*, **359**, 29 - 32.
- Manabe, S. & R.J. Stouffer, 1988, "Two stable equilibria of a coupled ocean-atmosphere model", *J. Climate*, **1**, 841 - 866.
- Manabe, S., R.J. Stouffer, M.J. Spelman and K. Bryan, "Transient Responses of a Coupled Ocean-Atmosphere Model to Gradual Changes of Atmospheric CO<sub>2</sub>. Part 1: Annual Mean Response", *Journal of Climate*, **4**, 785-818, 1991.
- Marth, P. C., J. R. Jensen, C. C. Kilgus, J. A. Perschy, J. L. MacArthur, D. W. Hancock, G. S. Hayne, C. L. Purdy, L. C. Rossi, and C. J. Koblinsky, Prelaunch Performance of the NASA Altimeter for the TOPEX/Poseidon Project, *IEEE Transactions on Geoscience and Remote Sensing*, Vol. 31, No. 2, March 1993, pp. 315-332.
- Martin, T.V., H.J. Zwally, A.C. Brenner and R.A. Bindshadler, 1983, "Analysis and retracking of continental ice sheet radar altimeter waveforms", *J. Geophys. Res.*, **88**, 1608 - 1616.
- Maykut, G.A., & N. Untersteiner, 1971, "Some results from a time-dependent thermodynamic model of sea ice", *J. Geophys. Res.*, **76**, 1550 - 1575.
- McAdoo, D., and S.W.Laxon, 1997, "Antarctic tectonics: Constraints from an ERS-1 Satellite Marine Gravity Field", *Science*, **276**, 556 - 560.
- McLaren, A.S., J.E. Walsh, R.H. Bourke, R.L. Weaver and W. Wittmann, 1992, "Variability in sea ice thickness over the North Pole from 1977-1990", *Nature*, **354**, 224-226.
- McLaren, A.S., R.H. Bourke, J.E. Walsh & R.L. Weaver, 1994, "Variability in sea ice thickness over the North Pole from 1958-1992", *Geophysical Monograph* **85**, 363 - 371, American Geophysical Union.
- Meier, M.F., 1984, "Contribution of small glaciers to global sea level", *Nature*, **343**, 115 - 116.
- Melbourne, W. G., E. S. Davis, T. P. Yunck & B. D. Tapley, 1994, "The GPS flight experiment on TOPEX/Poseidon", *Geophys. Res. Lett.*, **21**, 2171-2174.
- Monterfredini, E., F. Morelli, G. Picardi & R. Seu, 1995, "A non-coherent surface backscattering model for radar observation of planetary bodies and its application to cassini radar altimeter", *Planetary and Space Science*, **43**, Elsevier Science Ltd.

- Murphy, J.M. & J.F.B. Mitchell, 1995, "Transient Response of the Hadley Centre Coupled Model to increasing carbon dioxide. Part II. Temporal and Spatial evolution of patterns", *J. Climate*, **8**, 57 - 80.
- Nakada, M., & K. Lambeck, 1988, "The melting history of the late Pleistocene Antarctic ice sheet", *Nature*, 333, 36 - 40.
- Peacock, N.R., 1998, Ph. D. Thesis, University of London.
- Peacock, N.R., S.W. Laxon, R. Scharoo and W. Maslowski, 1997, "Improving the Signal to Noise Ratio of Altimetric Measurements in Ice Covered Seas", (Abstract), *EOS Trans. (Suppl.)*, **78**, F140.
- Peacock, N.R., S.W. Laxon, R. Scharoo, W. Maslowski and D.P. Winebrenner, 1998, "Geophysical signature from precise altimetric height measurements in the Arctic Ocean", *Proceedings IGARRS 98*, Seattle, Washington, pp.
- Peltier, W.R., 1988, "Global Sea Level and Earth Rotation", *Science*, **240**, 895 - 901.
- Phalippou, L., 1998, "Feasibility study of a high spatial resolution radar altimeter (HSSRA)", ESA Contract 12178/96/NL/SB(SC) Final Report
- Phalippou, L., P. Piau, D.J. Wingham & C. Mavrocordatos, 1998, "High resolution radar altimeter for ocean and ice sheet monitoring", *Proceedings IEEE International Geoscience and Remote Sensing Symposium IGARSS'98*, Seattle, Washington, USA, IEEE No. 98CH36174, July 1998, p 2020-2022.
- Picardi, G., R. Sen, and S. Sorge, Extensive Non-Coherent Averaging in Doppler Beam Sharpened Space-Borne Radar Altimeters, *Proc. IEEE Geoscience and Remote Sensing Symposium IGARSS'98*, Seattle, Washington, IEEE 98CH36174, July, 1998, pp. 2643-2645.
- Piexoto, J.P. & A.H. Oort, 1992, "The Physics of Climate", American Institute of Physics, New York.
- Raney, R. K., 1995, "A Delay/Doppler Radar for Ice Sheet Monitoring", *Proc. IEEE Geoscience and Remote Sensing Symposium IGARSS'95*, Florence, Italy, IEEE 95CH35770, July, 1995, pp. 862-864.
- Raney, R.K., 1995, "The Delay/Doppler Radar Altimeter", *IEEE Transactions on Geoscience and Remote Sensing*, **36**, No. 5, Sept 1998, pp. 1578-1588.
- Reeh, N., 1991, "Greenland ice sheet mass balance and sea level change" in *Glaciers, Ice Sheets and Sea Level: Effects of a CO<sub>2</sub> induced Climatic Change*, National Academy Press, Washington, 155 - 171.
- Rothrock, D.A. and A.S. Thorndike, 1984, "Measuring the Sea Ice Floe Size Distribution", *J. Geophys. Res.*, **89**, 6477-6486.
- Rott, H., P. Shvarka & T. Nagler, 1996, "Rapid Collapse of Northern Larsen Ice Shelf, Antarctica", *Science*, **271**, 788 - 792.
- Smith, D.M., C. Cooper, D.J. Wingham & S.W. Laxon, 1997, Evaluation of the representation of Arctic sea-ice in the UK Hadley Centre GCM, *Ann. Glaciology*, **25**, 423-428.
- Thomas, D., S. Martin, D. Rothrock & M. Steele, 1996, "Assimulating satellite concentration data into an Arctic sea ice mass balance model, 1979 - 1985", *J. Geophys. Res.*, **101**, 20849 -208868.
- Thomas, R.H., T.J.D. Sanderson & K.E. Rose, 1979, "Effects of a climatic warming on the West Antarctic Ice Sheet", *Nature*, **227**, 355 - 358.
-



- van der Veen, C.J., 1993, "Interpretation of short-term ice sheet elevation changes inferred from satellite altimetry", *Climatic Change*, **23**, 383 - 405.
- Varekamp, J.C., E. Thomas & O. Van de Plassche, "Relative Sea Level Rise and Climate Change over the Past 1500 years", *Terra Nova*, **4**, 293 - 304.
- Vinje, T., N. Nordlund and A. Kvambekk, 1998, "Monitoring ice thickness in the Fram Strait", *J. Geophys. Res.*, **103**, 10437-10449.
- Wadhams, P., 1990, "Evidence for the thinning of Arctic ice cover north of Greenland", *Nature*, **345**, 795-797.
- Wadhams, P., 1995, "Arctic sea ice extent and thickness", *Phil. Trans. Roy. Soc. Lond.*, **352**, 301-319.
- Wadhams, P., W.B. Tucker III, W.B. Krabill, R.N. Swift, J.C. Comiso and N.R. Davis, 1992, "Relationship Between Sea Ice Freeboard and Draft in the Arctic Basin, and Implications for Ice Thickness monitoring", *J. Geophys. Res.*, **97**, 20325-20334
- Wahr, J., H. DaZhong & A. Trupin, 1995, "Predictions of vertical uplift caused by changing volumes on a visco-elastic Earth", *Geophys. Res. Lett.*, **22**, 977-980.
- Wahr, J., C. Bentley & D.J. Wingham, 1998, "Estimating post-glacial rebound using GRACE and GLAS", *EOS Trans. (Abs.)*, in press.
- Walter, R.A. & M.F. Meier, 1989, "Variability of glacier mass balances in western North America" in *Aspects of Climate variability in the Pacific and western Americas*, *Geophysical Monograph* **55**, American Geophysical Union, 365 - 381.
- Warrick, R.A., C. Le Provost, M.F. Meier, J. Oerlemans & P.L. Woodworth, 1996, "Changes in Sea Level", in *Climate Change 1995, The Science of Climate Change*, Cambridge University Press.
- Weaver, A.J., & E.S. Sarachik, 1991, "Evidence for decadal variability in an ocean atmosphere circulation model: An advective mechanism", *Atmosphere-Ocean*, **29**, 197-231.
- Wingham, D.J., 1995, "Elevation change of the Greenland Ice Sheet", *Phil. Trans. Roy. Soc. Lond.*, **352**, 342 - 354.
- Wingham, D.J., 1995b, "A method for determining the average height of a large ice topographic ice sheet from observations of the echo received by a satellite altimeter", *J. Glaciology*, **41**, 125 - 141.
- Wingham, D.J., 1997, "High Resolution Altimeter Simulation Requirements", ESA Contract Report UCL-TA-TN-002.
- Wingham, D.J., 1998, "Short fluctuations in the mass, density and thickness of a dry firn column", submitted to *J. Glaciology*.
- Wingham, D.J., C.G. Rapley and H.D. Griffiths, 1986, "New techniques in satellite altimeter tracking systems", in *IGARSS' 86 Symposium Proceedings, Zurich*, ESA SP-245, pp 1339 - 1344.
- Wingham, D.J., A.J. Ridout, R. Scharroo, R.J. Arthern & C.K. Shum, 1998, "Antarctic Elevation Change 1992 to 1996", *Science*, **282**, 456 - 458
- WCRP, 1998, "Scientific Concept of the Arctic Climate System Study (ACSYS)", World Climate Research Program WMO/TD - No. 486.
- WCRP, 1998, "CLIVAR Initial Implementation Plan", World Climate Research Program WMO/TD - No. 869.
- Zelli, C., 1998, "High Spatial Resolution Radar Altimeter: Payload Options Definition", ESA Contract Report, TNO/RAS/0041/ALS Issue 2.



		Issue: 1 Date: 21. September 1999 Page: 50
---	--	--

Zwally, H.J., Parkinson, C.L., and Comiso, J.C., 1983, "Variation of Anatretic Sea Ice and Changes in carbon dioxide", *Science*, **220**, 1005 - 12.

Zwally, H.J., A.C. Brenner, J.A. Major, R.A. Bindshadler & J.G. Marsh, 1990, "Greenland Ice Sheet: Is it growing or shrinking?", *Science*, **248**, 288 - 289.